Thermal, Morphological and Spectroscopic Studies on Cellulose Modified with Phosphorus, Nitrogen, Sulphur and Halogens

RAJESH K. JAIN, KRISHAN LAL, and HARI L. BHATNAGAR,
Department of Chemistry, Kurukshetra University, Kurukshetra 132 119, India

Synopsis

The kinetics of the thermal degradation of cellulose and modified cellulose, namely, cellulose phosphate, cellulose carbanilate, cellulose tosylate, chlorodeoxycellulose, bromodeoxycellulose, and iododeoxycellulose in air were studied by thermogravimetry and differential thermal analysis from ambient temperature to 700°C. The various thermodynamic functions for different stages of thermal degradation had been obtained following the procedure of Broido. The activation energies for the oxidative decomposition of cellulose and modified celluloses were found to be in the range 30–399 kJ mol^{-1}. The infrared spectra of the residues of modified celluloses gave indication of formation of a compound containing P=O, P—O—P (only in the case of cellulose phosphate), C=C, and C=O groups in the final residual char. The EPR signals indicated the formation of trapped and stable free radicals in the thermal degradation of all the compounds, particularly halodeoxycelluloses showed generation of large amounts of trapped free radicals during the oxidative decomposition. Scanning electron micrographs of the thermally degraded cellulose derivatives show changes in the fibrillar structure, evolution of gaseous products, and film formation depending upon the nature of the substituent in the cellulose matrix. The mechanism of thermal degradation of these compounds has been proposed.

INTRODUCTION

Cotton cellulose is one of the textile materials frequently cited as causing burn injuries. However, it is easily rendered flame resistant by application of proper flame retardants. Some of the most successful flame retardants for polymer have been the compounds containing phosphorus, nitrogen, sulfur, and halogens in different combinations.[1,2] Of these, phosphorus, nitrogen, and halogen compounds have been extensively studied in cellulosic polymers.[3,4] In these polymers, the most important effect is to increase the char content and thus produce a lower percentage of flammable volatiles. Nearly all phosphorus and halogen compounds that decompose to acid fragments at low temperature are effective as flame retardants. These increase the rate of thermal degradation of the material at a given low temperature thereby reducing its heat stability.[5,6] Nitrogen and sulfur in combination with phosphorus also show a synergistic effect.[7,8] The thermal degradation of cellulose itself and chemically modified cellulose with these elements (i.e., P, N, S, halogens) have been investigated, but only few attempts have been made to study their morphology and kinetics of thermal degradation.

In this article, cellulose modified with phosphorus, nitrogen, sulfur, halogens, and their combinations was prepared and the kinetics of the thermal

Journal of Applied Polymer Science, Vol. 33, 247–282 (1987)
 CCC 0021-8995/87/020247-36$04.00

degradation were studied from ambient temperature to 700°C using thermogravimetry (TG), differential thermogravimetry (DTG), and differential thermal analysis (DTA) techniques. Morphology of cellulose and modified cellulose in the thermal decomposition range was studied by scanning electron microscopy (SEM) technique. Further, the composition of the charred products was studied by IR and EPR spectra of chars obtained at various temperatures.

EXPERIMENTAL

The following samples of cellulose and its derivatives containing phosphorus, nitrogen, sulfur, and halogens were selected for the present work. Sample (i): cellulose (from Schleicher and Schüll, Kassel, West Germany), dried to a constant weight *in vacuo* at 60°C; sample (ii): cellulose phosphate was prepared by treating cellulose with salt of *N*-phosphoryl-*N'*-methylimidazole[9] at 80°C for 24 h. The product was concentrated and the residue was dissolved in 95% ethanol and further precipitated with aniline. A yellow precipitate of anilinium salt of cellulose phosphate was filtered, washed thoroughly with water, and dried over P_2O_5 *in vacuo*; sample (iii): cellulose carbanilate was prepared by treating cellulose with phenyl isocyanate in pyridine at 100°C for 6 h. The cooled mixture was poured in distilled water and the precipitate was digested in ethanol warmed to 40°C, filtered. The product was purified by extracting with methanol in Soxhlet extractor and dried in vacuo over P_2O_5; sample (iv): cellulose tosylate was obtained by treating cellulose with *p*-toluenesulphonyl chloride (tosyl chloride) in pyridine at 20°C for 240 h, precipitated and purified by the method of Heuser et al.;[10] samples (v-vii): chlorodeoxycellulose, bromodeoxycellulose, and iododeoxycellulose were prepared by detosyloxylation of cellulose tosylate on heating with anhydrous lithium chloride, sodium bromide and sodium iodide, respectively, in 2,4-pentanedione at 125°C for 7 h. The cooled mixture was poured in ethanol and the precipitated product was filtered. The product was purified by dissolving in pyridine and reprecipitation from water. It was Soxhlet extracted with acetone and dried *in vacuo*. The percent of P, N, S and halogens of different samples was determined[11,12] and are as follows: Cellulose phosphate P 5.15 and N 6.68%, cellulose carbanilate N 8.12%, cellulose tosylate S 10.53%, chlorodeoxycellulose Cl 5.52 and S 7.70%, bromodeoxycellulose Br 17.13 and S 5.54%, and iododeoxycellulose I 43.47% and S 0.70%. It may be mentioned that partial detosylation takes place only in the case of halodeoxycelluloses.

Thermal Analysis. The DTA, TG, and DTG thermograms were obtained using a MOM derivatograph (Paulik, Paulik and Erdey, Budapest, Hungary). The DTA and TG curves were run under a dynamic air (dried) atmosphere flowing at 100 mL/min and at a scanning rate of 10°/min. The DTA measurements were related to calcined alumina.

Infrared Spectroscopy. For the IR studies (Beckman Spectrophotometer IR-20, USA), the charred samples of cellulose and its derivatives containing phosphorus, nitrogen, sulfur, and halogens were prepared by the KBr technique using 2% char. The charred samples were prepared by heating them in DTA cell in air (dried) atmosphere. Heating was stopped at the desired

temperature and the residues were allowed to cool and quickly transferred to a stoppered sample container.

Electron Paramagnetic Resonance Spectroscopy. Electron paramagnetic resonance spectra of charred samples of cellulose and modified cellulose, containing phosphorus, nitrogen, sulfur, and halogens were recorded on a Varian E-112 EPR spectrometer operating at 9.45 GHz with a field modulation of 100-kHz and 100 mg of charred sample was taken in the sample tube for each measurement. The 1,1-diphenyl-2-picryl hydrazyl (DPPH) signal was used as a standard for g values.

Scanning Electron Microscopy. Scanning electron microscopy (SEM) observations were made using a Philips PSEM-500 instrument operated at an emission current of 20 kV and 20 μA with the specimen position tilted at 33.5° and a pressure of about 10^{-5} mmHg. Samples for SEM were mounted on metal stubs with adhesive tape and were sputtered with gold.

RESULTS AND DISCUSSION

Thermal analysis of (i) cellulose, (ii) cellulose phosphate, (iii) cellulose carbanilate, (iv) cellulose tosylate, (v) chlorodeoxycellulose, (vi) bromodeoxycellulose, and (vii) iododeoxycellulose were carried out in air atmosphere from

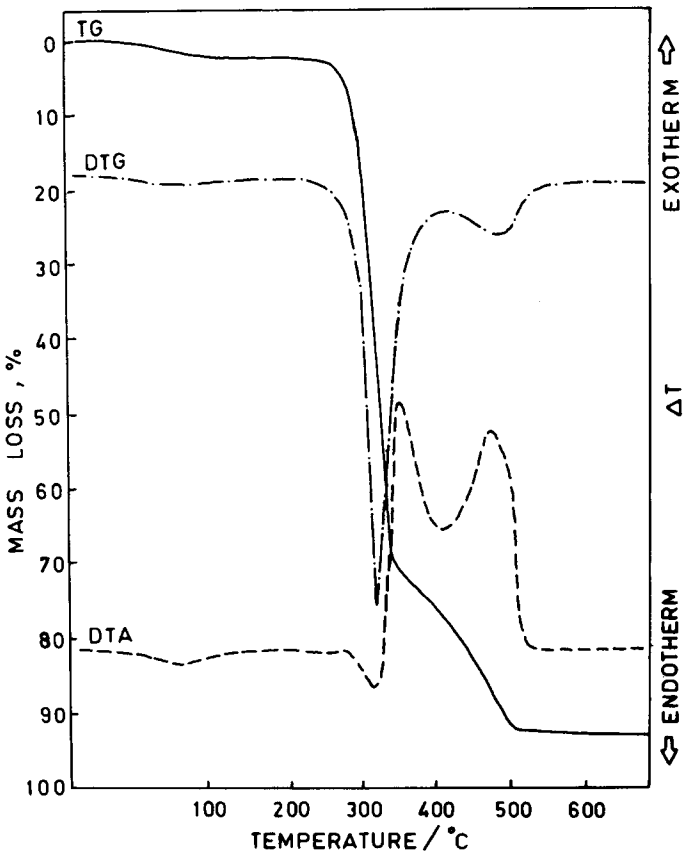

Fig. 1. Thermal analysis of cellulose in air.

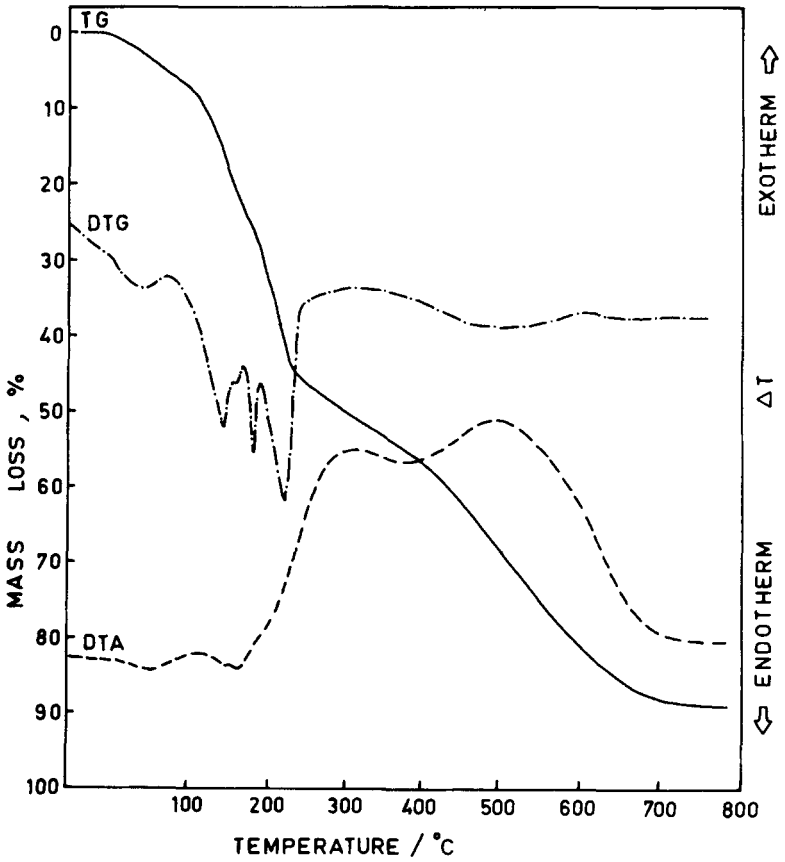

Fig. 2. Thermal analysis of cellulose phosphate in air.

ambient temperature to 700°C and are shown in Figures 1–7. The peak temperatures for various endotherms and exotherms were measured and are given in Table I. In some of the compounds, an endotherm observed below 100°C is due to the evaporation of moisture. The DTA curve of cellulose shows weak exothermic reaction with peaking at 274°C followed by an endotherm at 314°C. The endotherm can be attributed to dehydration and depolymerization leading to formation and evaporation of flammable volatile products and the next large exotherm peaking at 350°C may be due to oxidation of these products. The last large exotherm maximum at 468°C represents oxidation of the charred residues. The high-molecular-weight charred residues[13] start to burn in air about 405°C and glowing is complete at 520°C with a char yield of 7.8% as shown in TG (Fig. 1.).

For cellulose phosphate (its anilinium salt), the initial two small endotherms in the temperature range 114–180°C and peaking at 142 and 159°C are associated with the splitting of aniline and dephosphorylation reactions. The released phosphorous acid catalyzes the decomposition of the residual cellulose, thereby minimizing the depolymerization that produces flammable tars, such as levoglucosan, and stimulating dehydration reaction at lower

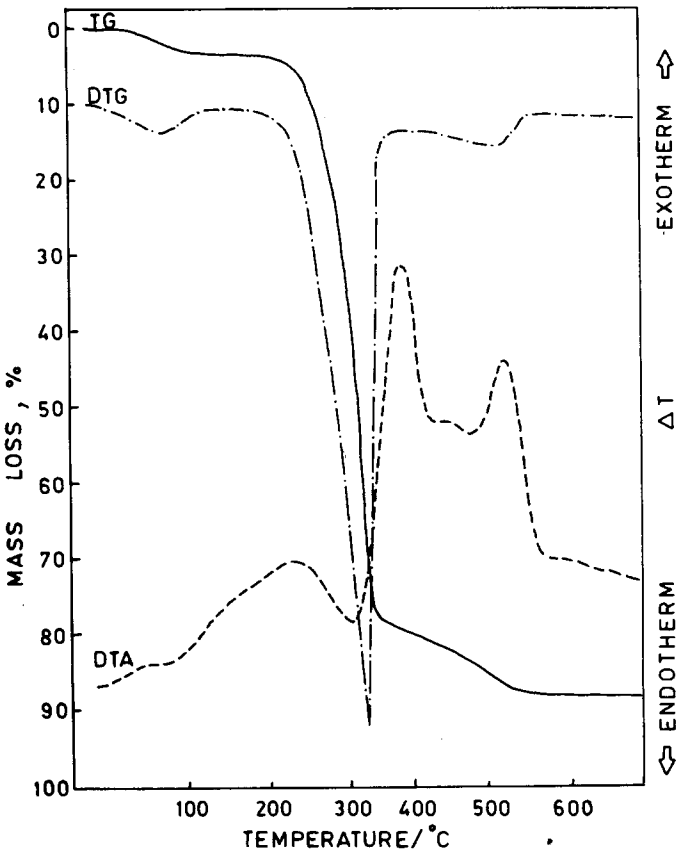

Fig. 3. Thermal analysis of cellulose carbanilate in air.

temperatures. The large mass loss of 18.3% in this temperature range in TG analysis supports this observation. The exotherm in the temperature range 180–380°C and peaking at 310°C is associated with the oxidative decomposition of the products. The last exotherm maximum at 500°C is due to oxidation of the charred residues.

The typical DTA thermogram of cellulose carbanilate shows an exotherm in the temperature range 85–303°C with peaking at 223°C. This may be visualized as resulting from the glass transition[14] accompanied by decomposition of cellulose carbanilate. The TG curve shows a mass loss of 34.5% in this temperature range. The next large exotherm in the temperature range 303–421°C with peaking at 382°C may be visualized due to the oxidative decomposition of the residual cellulose. The last large exotherm peaking at 524°C as usual is due to the oxidation of charred residues.

However, the cellulose tosylate, chlorodeoxycellulose, bromodeoxycellulose, and iododeoxycellulose containing S, Cl and S, Br and S, and I and S, respectively, decompose at significantly lower temperatures than those found in the decomposition of cellulose. For cellulose tosylate, a drift in the DTA curve observed with a little mass loss at 144°C is followed by two exothermic

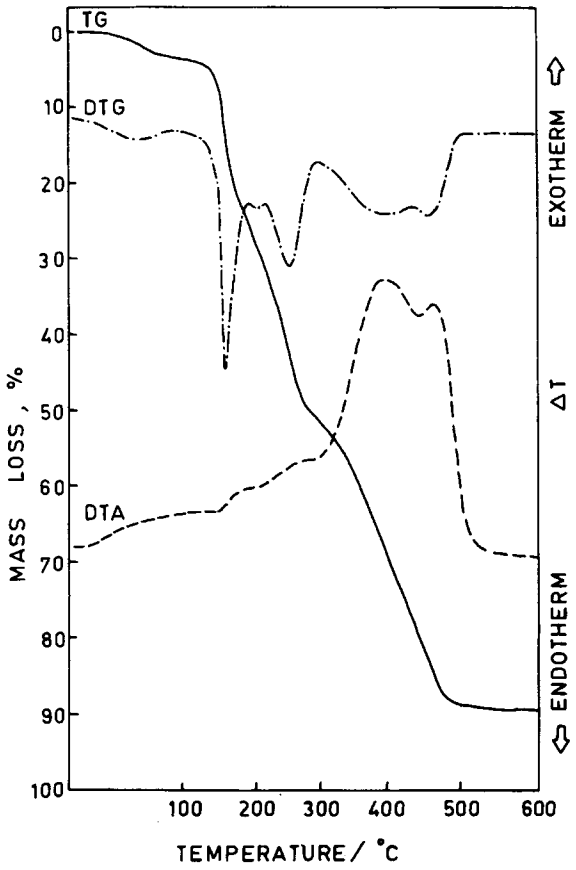

Fig. 4. Thermal analysis of cellulose tosylate in air.

reations peaking at 182 and 270°C in the temperature range 144–295°C which may be due to the oxidative decomposition of the cellulose tosylate accompanied by scission of tosyl group. The scission of tosyl group from cellulose tosylate should give an endotherm; but this probably merges with the exotherms due to simultaneous decomposition of the compound. This is supported by a large mass loss of 44.7% in this temperature range as shown by TG curve (Fig. 4). The next two large exotherms in the temperature range 295–440°C and 440–550°C are due to oxidation of aliphatic and aromatic charred residues, respectively.

For chloro-, bromo-, and iododeoxycellulose, the exotherms observed for these compounds at 205°C (180–220°C), 191°C (170–215°C), and 181°C (155–210°C) are due to oxidative decomposition of the products catalyzed by released acids.[15] It can be seen that the decomposition temperature decreases continuously in the order: chlorodeoxycellulose > bromodeoxycellulose > iododeoxycellulose, indicating that the thermal stability of these compounds decreases with increasing size of the substituent in the cellulose matrix. The next small exotherms for chloro-, bromo-, and iododeoxycellulose in the temperature ranges 220–300°C, 215–300°C, and 210–290°C, respectively, are

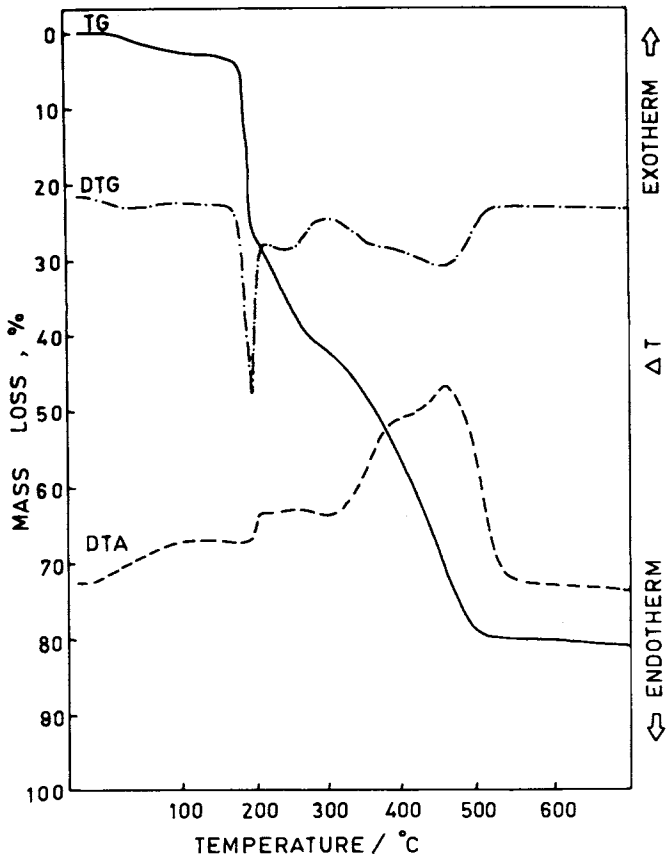

Fig. 5. Thermal analysis of chlorodeoxycellulose in air.

due to decomposition of the residual products. The last large exotherms for these compounds with peaking at 462, 466, and 471°C represent the oxidation of charred residual products.

The mass versus temperature curves for cellulose and its derivatives containing phosphorus, nitrogen, sulfur, and halogens are shown in Figures 1–7. In some cases, the initial but small mass loss due to absorbed moisture was neglected. The kinetic parameters for various stages of thermal degradation were determined using the method described by Broido.[16] The equation involved in Broido method can be written as

$$\ln\left(\ln\frac{1}{y}\right) = -\frac{E_a}{R}\cdot\frac{1}{T} + \ln\left(\frac{R}{E_a}\cdot\frac{Z}{RH}\cdot T_m^2\right) \tag{1}$$

where y is the fraction of the number of initial molecules not yet decomposed, T_m is the temperature of maximum reaction velocity, RH is the rate of heating, and Z is the frequency factor.

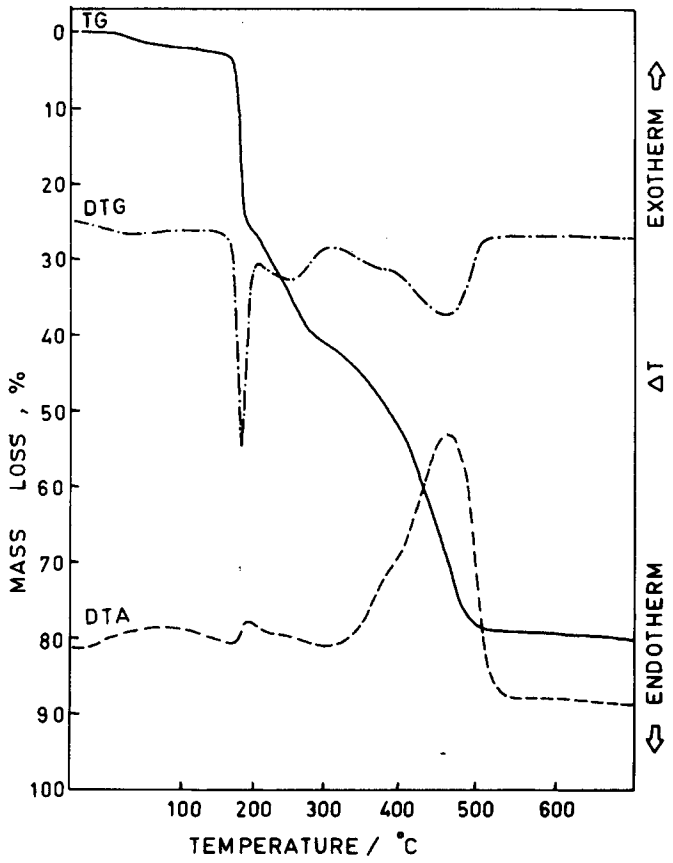

Fig. 6. Thermal analysis of bromodeoxycellulose in air.

Using Broido's method, plots of $\ln(\ln 1/y)$ versus $1/T$ for various stages of thermal degradation are given in Figures 8–11. The values of the activation energies, E_a and the frequency factors, Z determined from the slopes and intercepts of these plots, respectively, are given in Tables II–V. These parameters have been evaluated using the method of least squares.

Table II shows that the temperatures for the detosylation and dehydrohalogenation for cellulose tosylate, chloro-, bromo-, and iododeoxycellulose appreciably decrease in comparison to that for dehydration for cellulose indicating that the introduction of sulfur and halogens in cellulose matrix decreases its heat stability. Further, it is observed that for first stage of thermal degradation of cellulose carbanilate, cellulose tosylate, chloro-, bromo-, and iododeoxycellulose, the activation energies reduce to 95, 88, 145, 137, and 124 kJ mol^{-1}, respectively, from 172 kJ mol^{-1} for cellulose. For cellulose phosphate, the lowering of decomposition temperature is so high that dephosphorylation and decomposition of cellulose phosphate occur simultaneously.

Table III gives the activation energies and frequency factors for the second stage of thermal degradation of cellulose and its derivatives. The thermogram of cellulose phosphate indicates three DTG maxima at 143, 179, and 222°C,

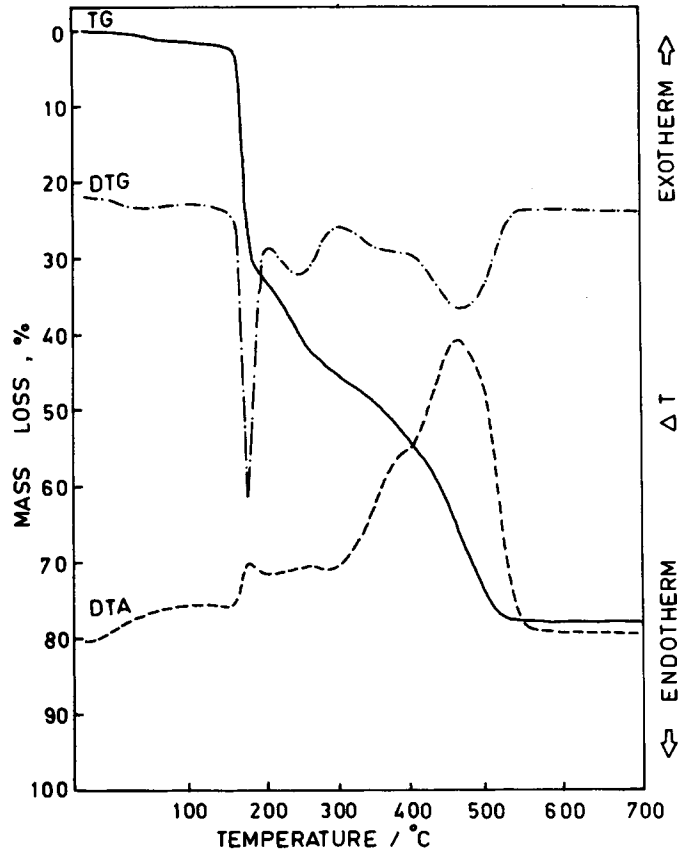

Fig. 7. Thermal analysis of iododeoxycellulose in air.

showing thereby that different reactions, namely elimination of aniline, dephosphorylation, and decomposition are occurring during second-stage thermal degradation. The activation energies for these processes are 60, 30, and 44 kJ mol^{-1}, respectively which are much lower as compared to the value of cellulose (238 kJ mol^{-1}). For cellulose carbanilate, the mass loss in the temperature range 255–340°C with DTG maximum at 325°C is about 69%. This is due to the decomposition of cellulose carbanilate with the release of phenyl isocyanate and cellulose moiety. The activation energy for this latter step decreases to 99 from 238 kJ mol^{-1} for untreated cellulose. The DTG curve for cellulose tosylate shows two maxima at 158 and 252°C; the first may be due to decomposition of the released *p*-toluenesulfonic acid, a strong dehydrating agent, and the second to the decomposition of the residual products. The activation energies due to oxidative decomposition of cellulose tosylate for these processes are 151 and 54 kJ mol^{-1}. For chloro-, bromo-, and iododeoxycellulose, the activation energies for decomposition are 353, 384, and 399 kJ mol^{-1}, respectively, which are much higher than the value of 238 kJ mol^{-1} for cellulose. The higher activation energies for decomposition of these

TABLE I
Peak Temperatures in the DTA Thermograms for Cellulose and Modified Celluloses containing Phosphorus, Nitrogen, Sulfur, and Halogens in Air

Sample no.	Compound	DTA curve			Nature of the DTA peak	
		Initiation temp./°C	Peak temp./°C	Termination temp./°C		
(i)	Cellulose	260	274	280	exo	(small)
		280	314	325	endo	(large)
		325	350	405	exo	(large)
		405	468	520	exo	(large)
(ii)	Cellulose phosphate	114	142	149	endo	(small)
		149	159	180	endo	(small)
		180	310	380	exo	(large)
		380	500	730	exo	(large)
(iii)	Cellulose carbanilate	85	223	303	exo	(large)
		303	382	421	exo	(large)
		476	524	575	exo	(large)
(iv)	Cellulose tosylate	144	182	200	exo	(small)
		200	270	295	exo	(small)
		295	392	440	exo	(large)
		440	461	550	exo	(large)
(v)	Chlorodeoxy-cellulose	180	205	220	exo	(small)
		220	250	300	exo	(small)
		300	462	555	exo	(large)
(vi)	Bromodeoxy-cellulose	170	191	215	exo	(small)
		215	257	300	exo	(small)
		300	466	560	exo	(large)
(vii)	Iododeoxy-cellulose	155	181	210	exo	(small)
		210	270	290	exo	(small)
		290	471	575	exo	(large)

compounds may be due to crosslinking taking place in the halogen derivatives which bring about an additional thermal degradation path, different from that leading to levoglucosan and necessitating a higher activation energy. The scanning electron micrographs of residues of chloro-, bromo-, and iododeoxy-cellulose also confirm these observations and will be discussed later.

After the decomposition stage, the residual materials of the cellulose and its derivatives containing phosphorus, nitrogen, sulfur, and halogens are found to degrade slowly in the temperature range 215–390°C. The activation energies and frequency factors for the third stage of thermal degradation are listed in Table IV. The energies of activation are in the range of 20–41 kJ mol^{-1}.

High temperature exotherms > 330°C in air atmosphere for cellulose and its derivatives (fourth stage) are due to oxidation of char residues. The activation energies and other parameters for this stage are presented in Table V.

To compare the flame-retardant properties of these compounds, the char yields (in mass %) were determined at 875 K from TG curves and are given in

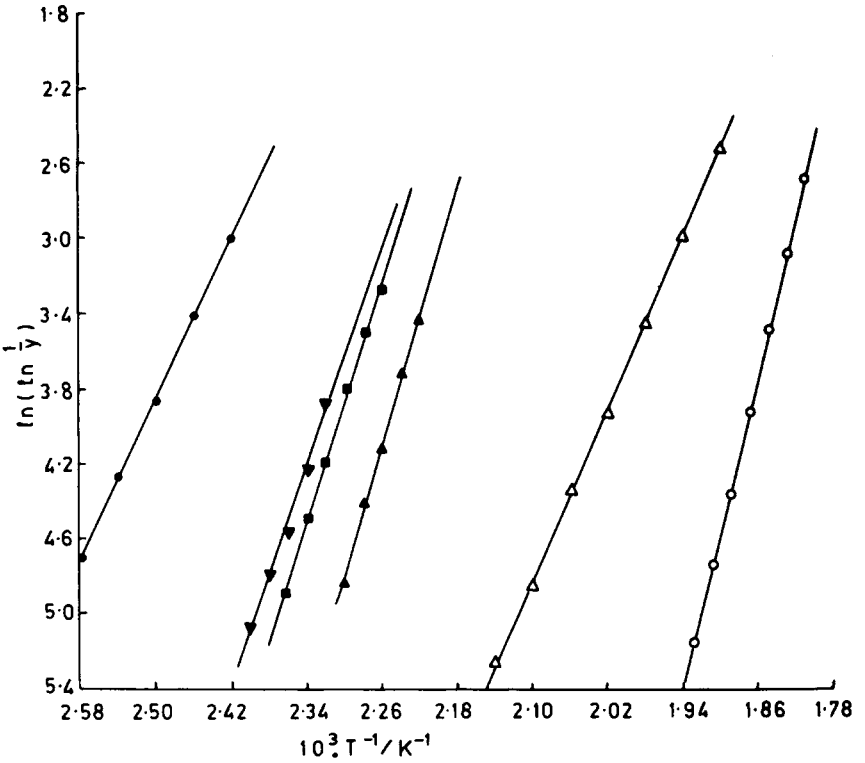

Fig. 8. Plots of $\ln(\ln 1/y)$ vs. $10^3 \cdot T^{-1}/K^{-1}$ using Broido equation for cellulose (○), cellulose carbanilate (△), cellulose tosylate (●), chlorodeoxycellulose (▲), bromodeoxycellulose (■), and iododeoxycellulose (▼) in air for first stage of thermal degradation.

Table V. It is evident from the char yields of cellulose carbanilate and cellulose tosylate that these compounds give higher char yields (12.4 and 10.7%, respectively) as compared to cellulose (7.8%), indicating the flame-retarding properties of these compounds. Further, cellulose phosphate, chloro-, bromo-, and iododeoxycellulose still show much higher char yields (19.2–22.6%), thus, diminishing the formation of flammable volatile products.

IR AND EPR SPECTRA OF CHARS

To understand the flaming combustion of cellulose and its derivatives, the char residues obtained at different temperatures (125–400°C) from unmodified cellulose and cellulose treated with phosphorus, nitrogen, sulfur, and halogens containing flame retardants were analyzed by IR and EPR. The changes in the IR spectra of chars of cellulose and modified celluloses are as follows. At lower temperatures (125–250°C) where an initial mass loss in TG is observed, the decrease of intensity of the hydroxyl stretching vibration bands (3450, 3350, and 3305 cm^{-1}) and the bands at 3020 (=C—H str), 2940 (—C—H str), 1360, 1190 and 1170 (C—SO_2—O—C str), 2590 (P—OH str), and 1250 (P=O

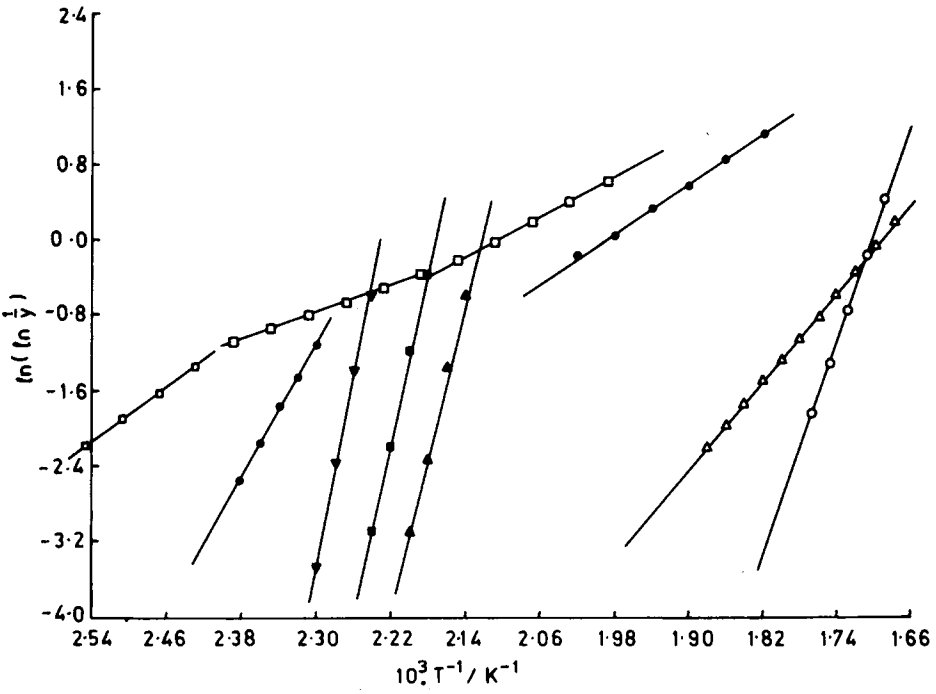

Fig. 9. Plots of $\ln(\ln 1/y)$ vs. $10^3 \cdot T^{-1}/K^{-1}$ using Broido equation for cellulose (○), cellulose phosphate (□), cellulose carbanilate (△), cellulose tosylate (●), chlorodeoxycellulose (▲), bromodeoxycellulose (■), and iododeoxycellulose (▼) in air for second stage of thermal degradation.

str) indicate that the dehydration and elimination of acid take place during the initial reaction of thermal degradation of cellulose and its derivatives. At elevated temperatures, the intensity of all the normal bands due to cellulose and its derivatives decrease and bands at 1720 (C=O) and 1630 cm^{-1} (C=C) appear, indicating that the skeletal rearrangement and the evolution of volatile products commence at elevated temperatures. At higher temperature (400°C), Figure 12 shows that the bands due to untreated and treated cellulose almost disappear and the absorption bands at 1720 (C=O), 1250 (P=O), and near 1000 cm^{-1} (C=C) become intense and the absorption band at 1630 cm^{-1} shifts to 1600 cm^{-1} (due to conjugated C=C) suggesting the extension of conjugation of the C=C bonds in the residues from cellulose and modified cellulose and the formation of compounds containing P=O (only for cellulose phosphate) and C=O groups. Further at this temperature, the cellulose phosphate shows a new absorption band at 950 cm^{-1} (due to pyrophosphate P—O—P linkage) indicating the formation of pyrophosphate compound in the final mass loss region of cellulose phosphate.

EPR spectra of chars of pure cellulose and modified cellulose compounds are shown in Figure 13. EPR spectra of chars of cellulose phosphate, cellulose tosylate, chloro-, bromo-, and iododeoxycellulose were obtained at 250°C in the air medium, whereas those of cellulose and cellulose carbanilate were

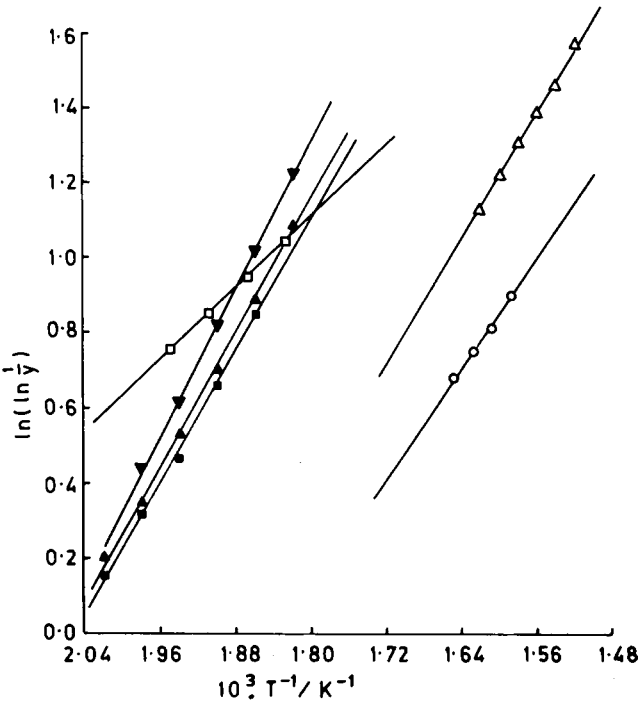

Fig. 10. Plots of $\ln(\ln 1/y)$ vs. $10^3 \cdot T^{-1}/K^{-1}$ using Broido equation for cellulose (○), cellulose phosphate (□), cellulose carbanilate (△), chlorodeoxycellulose (▲), bromodeoxycellulose (■), and iododeoxycellulose (▼) in air for third stage of thermal degradation.

obtained at 300°C due to their higher decomposition temperatures. The relative intensities of the EPR spectral lines were computed by measuring the peak-to-peak derivative amplitude and peak-to-peak width of the derivative spectral line using the method described by Wertz and Bolton.[17] The relative intensities, thus calculated by this procedure and hence the relative concentration of free radicals[18] of the chars of cellulose, cellulose phosphate, cellulose carbanilate, cellulose tosylate, chloro-, bromo-, and iododeoxycellulose are found to be in the ratio of 1.0 : 0.1 : 0.7 : 0.5 : 2.2 : 3.0 : 3.7, respectively. It is obvious that there is formation of trapped free radicals[19] to a small extent during the decompostion of cellulose. Further, the formation of free radicals is associated with char formation during decomposition of a compound.[20] As the number of free radicals formed is small for cellulose, little char is obtained during the thermal degradation of cellulose. For cellulose phosphate, too, the number of free radicals generated is very small, one should expect little char production for this compound. But this is not so. The char yield for cellulose phosphate is very high due to different thermal degradation mechanism as discussed later. For cellulose carbanilate and cellulose tosylate, the EPR spectra of chars show formation of small number of free radicals during the decomposition. So the char yields for these compounds are also low as expected.

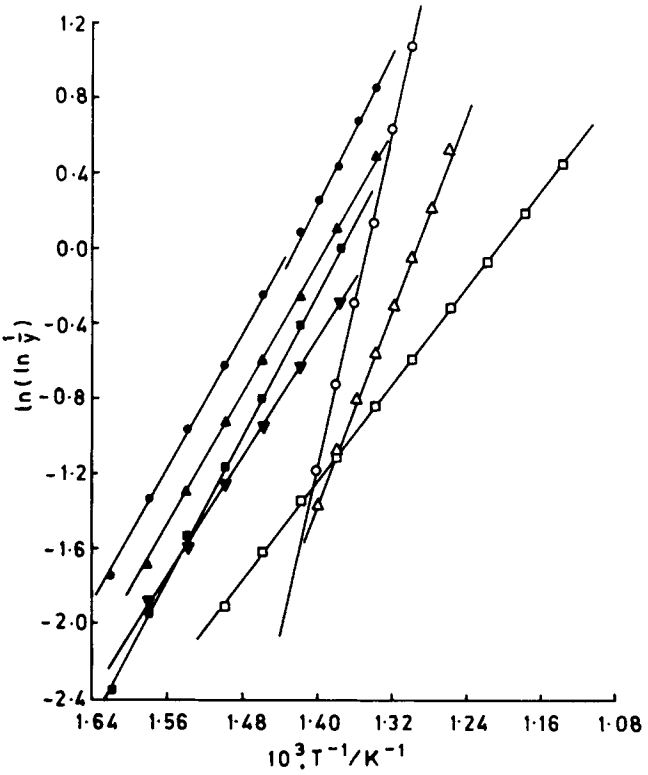

Fig. 11. Plots of $\ln(\ln 1/y)$ vs. $10^3 \cdot T^{-1}/K^{-1}$ using Broido equation for cellulose (○), cellulose phosphate (□), cellulose carbanilate (△), cellulose tosylate (●), chlorodeoxycellulose (▲), bromodeoxycellulose (■), and iododeoxycellulose (▼) in air for fourth stage of thermal degradation.

TABLE II
Activation Energies and Frequency Factors for First Stage of Thermal Degradation of Cellulose and Modified Celluloses Containing Phosphorus, Nitrogen, Sulfur, and Halogens in Air (Broido Method)

Sample no.	Compound	Temperature range/°C	E_a/kJ mol^{-1}	Z/s^{-1}
(i)	Cellulose	240–285	172.1	1.36×10^{13}
(ii)	Cellulose phosphate	—	—	—
(iii)	Cellulose carbanilate	190–255	95.4	1.63×10^{6}
(iv)	Cellulose tosylate	110–145	87.6	5.98×10^{7}
(v)	Chlorodeoxycellulose	160–180	145.3	3.36×10^{13}
(vi)	Bromodeoxycellulose	150–170	136.6	7.58×10^{12}
(vii)	Iododeoxycellulose	140–160	124.1	2.89×10^{11}

TABLE III
Activation Energies and Frequency Factors for Second Stage of Thermal Degradation of Cellulose and Modified Celluloses containing Phosphorus, Nitrogen, Sulfur, and Halogens in Air (Broido Method)

Sample no.	Compound	DTG maxima/ °C	Temperature range/°C	E_a/kJ mol^{-1}	Z/s^{-1}
(i)	Cellulose	321	285–335	238.4	2.18×10^{19}
(ii)	Cellulose phosphate	143	100–145	60.2	7.98×10^{4}
		179	145–185	29.7	5.05
		222	185–235	43.6	2.25×10^{2}
(iii)	Cellulose carbanilate	325	255–340	99.1	3.18×10^{6}
(iv)	Cellulose tosylate	158	145–180	150.7	7.01×10^{15}
		252	210–280	54.4	1.78×10^{3}
(v)	Chlorodeoxycellulose	196	180–205	352.6	4.61×10^{37}
(vi)	Bromodeoxycellulose	184	170–195	384.4	1.58×10^{42}
(vii)	Iododeoxycellulose	175	160–185	399.0	1.18×10^{45}

TABLE IV
Activation Energies and Frequency Factors for Third Stage of Thermal Degradation of Cellulose and Modified Celluloses containing Phosphorus, Nitrogen, Sulfur, and Halogens in Air (Broido Method)

Sample no.	Compound	Temperature range/°C	E_a/kJ mol^{-1}	Z/s^{-1}
(i)	Cellulose	335—370	30.4	1.34
(ii)	Cellulose phosphate	235—280	19.9	3.51×10^{-1}
(iii)	Cellulose carbanilate	340—390	36.6	6.45
(iv)	Cellulose tosylate	—	—	—
(v)	Chlorodeoxycellulose	215—285	37.0	2.67×10^{1}
(vi)	Bromodeoxycellulose	215—280	34.2	1.23×10^{1}
(vii)	Iododeoxycellulose	215—280	40.7	7.48×10^{1}

For halodeoxycelluloses, EPR spectra indicate the generation of large numbers of relatively stable and trapped free radicals and that the number of free radicals increases progressively from chloro- to bromo- to iododeoxycellulose. Consequently, the char yield should be in the order iodo- > bromo- > chlorodeoxycellulose (Table V).

THERMAL DEGRADATION MECHANISM

The thermal degradation of cellulose proceeds by two alternative pathways. These pathways involve decomposition of the glycosyl units to form char, which dominates at lower temperatures and depolymerization of these units to form volatile tarry products containing levoglucosan, which dominates at higher temperatures. Oxidation of the volatiles in the gas phase gives flaming combustion, and oxidation of char in the solid phase, remaining after evaporation of the volatile products, produces smoldering or glowing combustion.

TABLE V
Activation Energies and Frequency Factors for Fourth Stage of Thermal Degradation of Cellulose and Modified Celluloses containing Phosphorus, Nitrogen, Sulfur, and Halogens in Air (Broido Method)

Sample no.	Compound	DTG maxima/°C	Temperature range/°C	E_a/kJ mol^{-1}	Z/s^{-1}	Char yield at 875K in mass %
(i)	Cellulose	482	425—500	187.1	1.03×10^{11}	7.8
(ii)	Cellulose phosphate	508	390—640	54.5	5.03	19.2
(iii)	Cellulose carbanilate	522	430—525	111.2	1.22×10^{5}	12.4
(iv)	Cellulose tosylate	398	330—430	77.4	2.17×10^{3}	10.7
		457	430—480	81.7	3.73×10^{3}	
(v)	Chlorodeoxy-cellulose	460	340—490	75.1	8.29×10^{2}	20.3
(vi)	Bromodeoxy-cellulose	462	340—480	81.2	2.18×10^{3}	20.9
(vii)	Iododeoxy-cellulose	470	340—500	68.5	1.66×10^{2}	22.6

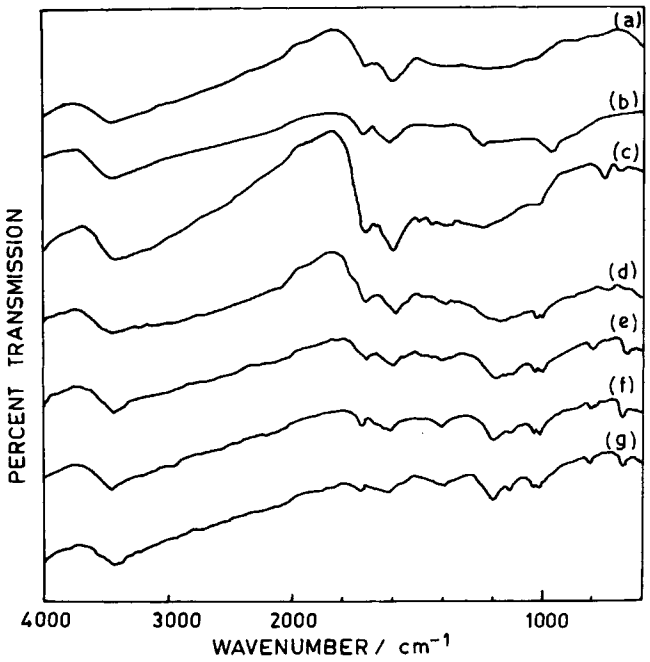

Fig. 12. IR spectra of chars of (a) cellulose, (b) cellulose phosphate, (c) cellulose carbanilate, (d) cellulose tosylate, (e) chlorodeoxycellulose, (f) bromodeoxycellulose, and (g) iododeoxycellulose at 400°C.

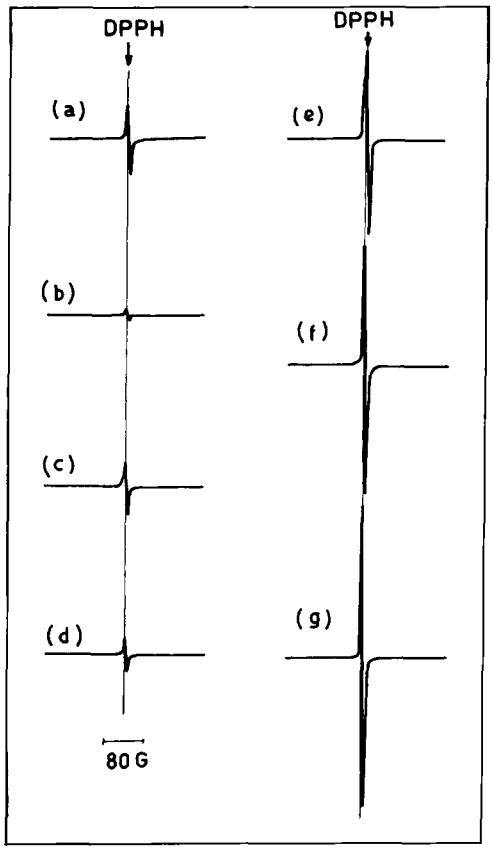

Fig. 13. EPR spectra of chars of (a) cellulose, 300°C, (b) cellulose phosphate, 250°C, (c) cellulose carbanilate, 300°C, (d) cellulose tosylate, 250°C, (e) chlorodeoxycellulose, 250°C, (f) bromodeoxycellulose, 250°C, and (g) iododeoxycellulose at 250°C.

The phosphorus compounds act as flame retardants for cellulose by lowering its temperature of decomposition, thereby favoring a dehydration pathway of decomposition as opposed to a depolymerization.[21,22]

In the case of cellulose, the phosphorus flame-retardant action occurs exclusively in the condensed phase.

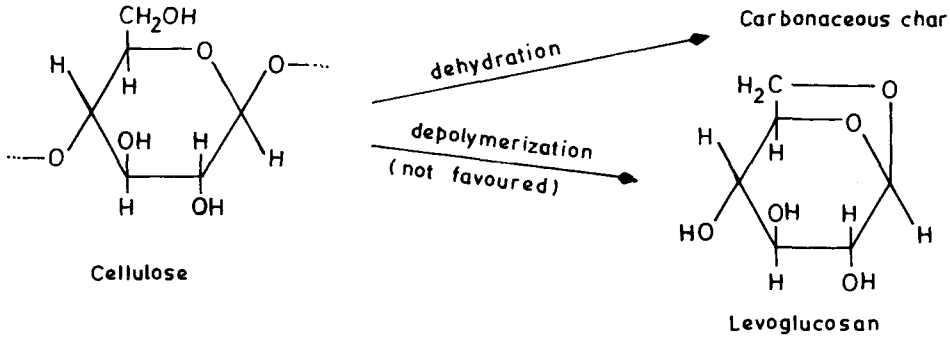

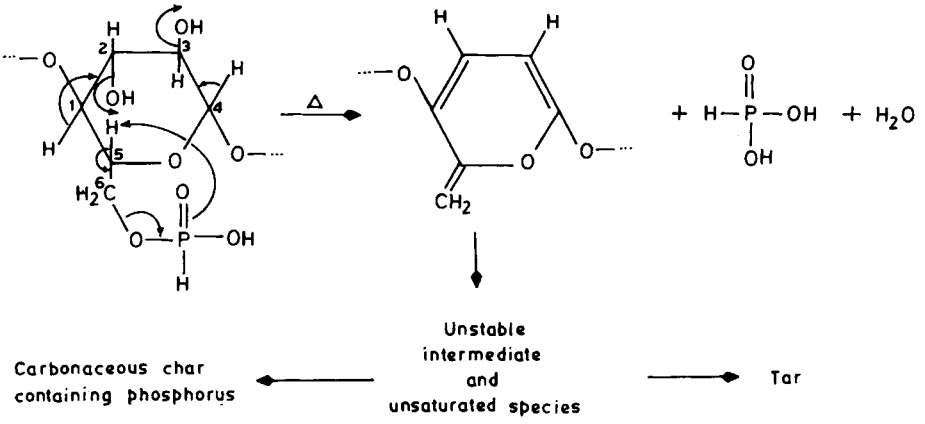

Scheme I

For cellulose phosphate (its anilinium salt) after the release of aniline at low temperature (100 ~ 150°C), the compound decomposes to acid fragments which catalyze oxidative decomposition to produce water and char. The dehydration may proceed according to Scheme I.

When heated to higher temperature, the phosphorous acid polymerizes to polyphosphorous acid which is more effective in catalyzing dehydration. The flame-retardant action of phosphorus compounds in cellulose proceeds by way of initial phosphorylation of the unreacted hydroxyl group of cellulose. Phosphorylated cellulose then breaks down to give water, phosphorous acid and an unsaturated cellulose analogue, eventually a nongraphitizing residue-containing phosphorus, by repetition of these steps.

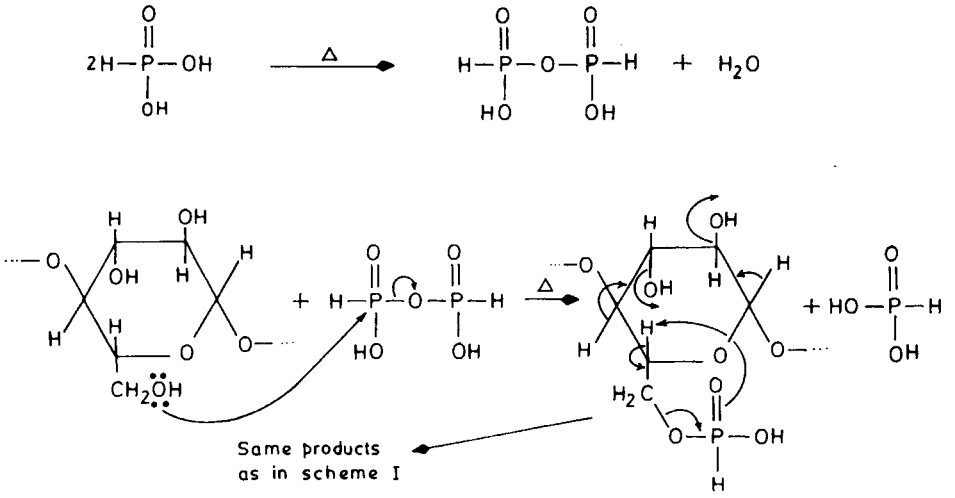

Scheme II

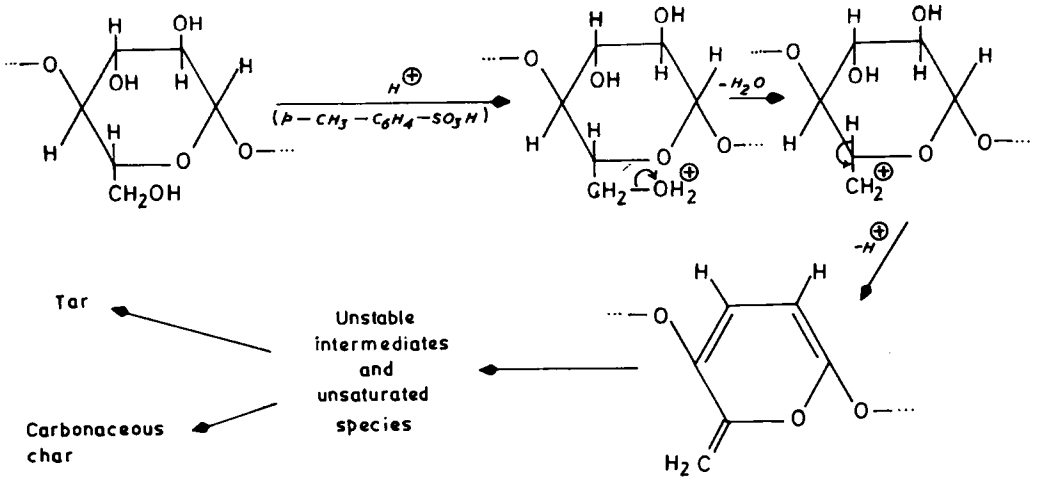

Scheme III

The detailed mechanism has been discussed elsewhere.[23] It is generally observed that in the case of phosphorylated cellulose, afterglow resulting from the oxidation of carbonaceous char is minimized due to the formation of a coating on the surface of cellulose residue by nonvolatile thermally stable polyphosphorous acid. Coating on the surface prevents the liberation of the volatile degradation products into the gas phase and thus results in the production of considerable char yield.

For cellulose carbanilate, the presence of nitrogen in cellulose is not particularly promising as good flame retardant as is evident from its high decomposition temperature and low char yield (Tables I and V). However, phosphorus-nitrogen synergism[24,25] seems to be useful for flame retardancy of cellulosic polymers.

On heating cellulose tosylate, a strong dehydrating agent (i.e., *p*-toluenesulfonic acid) is released initially. As the acid produced is very strong in comparison to phosphorous acid, it is believed that *p*-toluenesulfonic acid-type flame retardant may bring about dehydration involving the unreacted hydroxyl group. The reaction may take place through a carbonium ion.

Owing to the formation of unstable carbonium ion intermediate and the presence of strong acid (i.e., *p*-toluenesulfonic acid), the above reaction could be expected to proceed rapidly through all its steps. The unsaturated cellulose analogue further decomposes to yield tar and carbonaceous char as mentioned earlier.

On comparing the char yields produced in the case of cellulose phosphate and cellulose tosylate at 875 K, it is observed that the former gives much higher char yield (19.2%) as compared to that of the latter (10.7%). This indicates that polyphosphorous acid catalyzes the dehydration reaction to a greater extent at the elevated temperature leading to primarily water and almost noncombustible char. Further, at higher temperature, the polyphosphorous acid produced forms a viscous coating on the surface of cellulose

residue which screens the hot carbon from the air, thus producing a large amount of char. The higher efficiency of phosphorus flame retardant is also indicated from the observation that phosphorus from the flame retardant is largely or completely retained in the final residual char.[26,27]

It is postulated that flame retardation of cellulose by halogens apparently acts in the gas phase by interfering with free radical chain reaction in the flame.[2] These free radicals retard the gas-phase combustion kinetics and, therefore, inhibit the combustion process.

For chloro-, bromo-, and iododeoxycellulose (partially substituted with tosyl group), the initial thermal degradation reaction begins with dehydrohalogenation and detosylation. The released hydrohalogenated acid and *p*-toluenesulfonic acid then catalyze the crosslinking due to intermolecular dehydration, transglycosylation, and other condensation reactions. Finally, homolytic cleavage of the substituents on the carbon chain of the condensation products gives a large amount of carbonaceous char still containing trapped free radical.[15,28] The scanning electron micrographs of chars of halodeoxycelluloses also show that at low temperature, after initial evolution of gases, the crosslinking is taking place and EPR spectra of chars at 250°C, show that the charring reactions are accompanied with the formation of trapped and relatively stable free radicals. Further, it is observed from the DTA and TG thermograms that the initial degradation temperature decreases in the order chlorodeoxycellulose > bromodeoxycellulose > iododeoxycellulose. The bond energies[29] of C—I, C—Br, and C—Cl bonds are 209 ± 21, 280 ± 21, and 397 ± 29 kJ mol^{-1}, respectively. Since the bond strength of carbon-halogen bond decreases in the order C—Cl > C—Br > C—I; the C—I bond will break at a lower temperature than C—Br bond which in turn will break at a lower temperature than C—Cl bond. Consequently, iododeoxycellulose with weak C—I bond will generate more free radicals as compared to other halodeoxycelluloses. EPR spectra of the chars of halodeoxycelluloses at 250°C also show the generation of free radicals in the order C—I > C—Br > C—Cl (Fig. 13). Based on the findings that the chars of halodeoxycelluloses exhibit signals in the EPR spectra, the following free radical chain mechanism may be proposed:

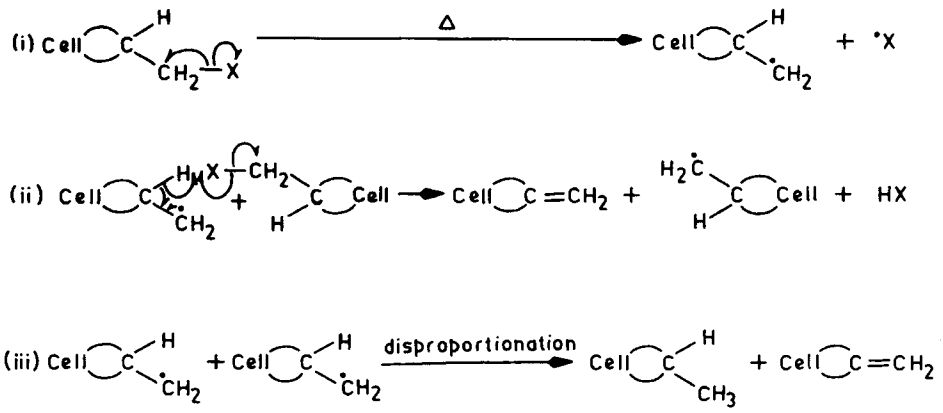

Since in none of the above steps a hydrogen atom, which accelerates the

burning process, is produced, a concerted propagation step (ii) seems to be quite reasonable for the suppression of the burning process. Hydrogen halide, thus released, exerts a further effect in producing the dehydration, condensation and charring reaction which have been shown to be acid catalyzed.[30]

MORPHOLOGY OF CELLULOSE AND CHEMICALLY MODIFIED CELLULOSES

In order to gain a better understanding of the structural modification of thermally degraded cellulose fiber and modified cellulose fiber at various temperatures, the scanning electron micrographs of the fibers and chars of thermally degraded fibers in the decomposition range were obtained. When viewed in SEM micrographs, pure cellulose fiber is seen as having a twisted, convoluted, ribbon-like structure with a furrowed surface [Fig. 14(a–b)]. Thus, at ×800 magnification, the micrograph [Fig. 14(a)], reveals convoluted cellulose fibers, although some fibrils are visible. However, at ×1600 magnification [Fig. 14(b)], the fibrils are clearly visible. These fibrils are potential reactive sites for a chemical reaction to take place with cellulose. The smooth surface generally offers greater resistance to chemical reactions. The scanning electron micrographs at ×800 and ×1600 magnifications of the residues of cellulose obtained at temperatures of 270, 310, and 350°C (near peak temperature in DTA) are shown in Figure 14(c–h). TG curve shows mass losses of 3.8, 40.3, and 69.5%, respectively at these temperatures. It is evident from Figure 14(c–d) that the cellulose fibers exposed to heat at 270°C for 15 min show decrease in fibrillation and they twist and curve in increasing order as the temperature is raised. However, even at 350°C where the mass loss is 69.5%, the char retains the basic morphological structure of cellulose fibers, although they become somewhat coarsened.

The SEM micrographs of cellulose phosphate show degradation at the microfibrillar sites [Fig. 15(a–b)]. When the sample is heated at 140, 180, and 260°C for 15 min [Fig. 15(c–h)], the twisting and shrivelling of fibers increase considerably. There is practically no indication of the evolution of the gases, showing thereby that the flame-retardant action of cellulose phosphate occurs in the condensed phase. The mass losses at the above temperatures are 11.6, 23.5, and 45.3%, respectively. In spite of large mass loss of 45.3% at 260°C, the fibrous structure of cellulose phosphate is retained [Fig. 15(g–h)].

SEM studies of cellulose carbanilate at magnifications of ×800 and ×1600 [Fig. 16(a–b)] show that alignment of the fibers takes place in the modified cellulose. The sample heated at 250, 300, and 350°C with corresponding mass losses in TG curve to be 4.6, 32.0, and 76.4%, respectively, show evidence of gas evolution as considerable pitting, shrinking and twisting take place [Fig. 16(c–h)]. The large mass loss at 350°C and pitting on the SEM micrographs indicate that large amount of gaseous products are being released on heating cellulose carbanilate.

The SEM micrograph of cellulose tosylate at ×800 magnification [Fig. 17(a)] shows degradation of cellulose structure and considerable decrease in fibrillation. The fibers show strong tendency towards alignment when heated at 150°C for 15 min [Fig. 17(b)]. At 175°C, the micrograph [Fig. 17(c)] shows a tendency of film formation and at a higher temperature of 200°C [Fig. 17(d)],

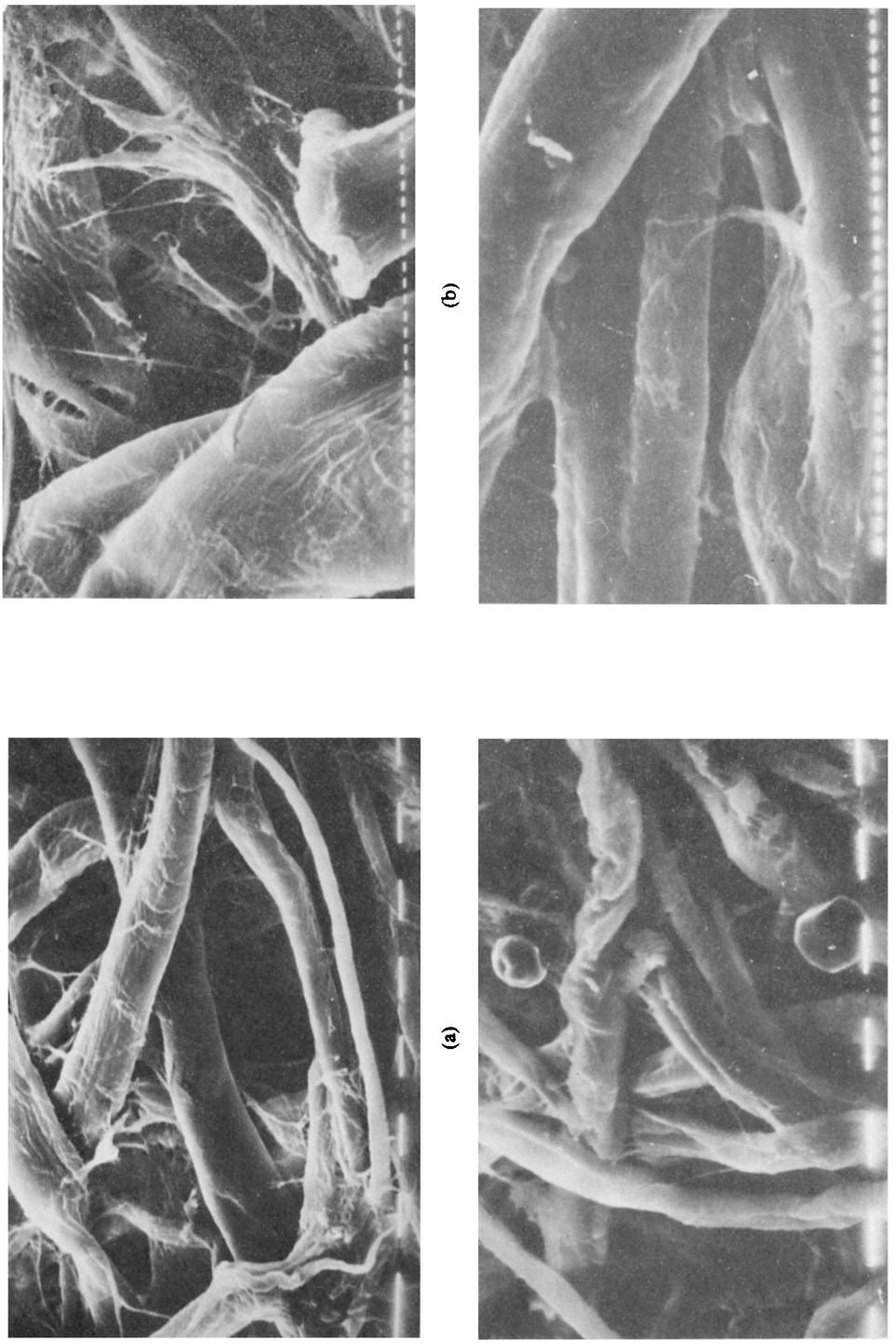

Fig. 14. Scanning electron micrographs of cellulose, (a) ×800, (b) ×1600, and cellulose heated for 15 min at (c) 270°C, ×800, (d) 270°C, ×1600, (e) 310°C, ×800, (f) 310°C, ×1600, (g) 350°C, ×800, and (h) 350°C, ×1600.

(f)

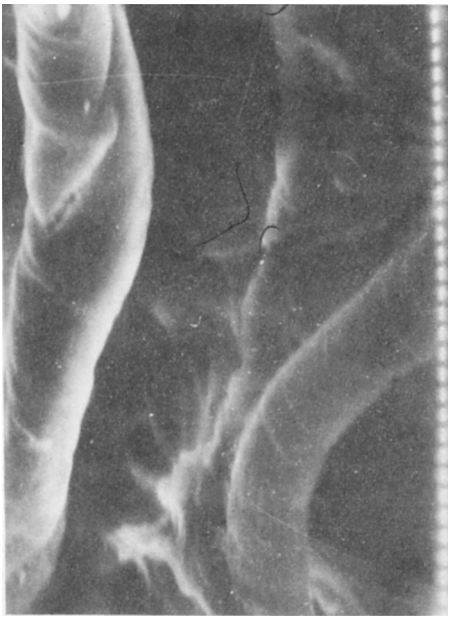

(h)

(e)

(g)

Fig. 14. *(Continued from the previous page.)*

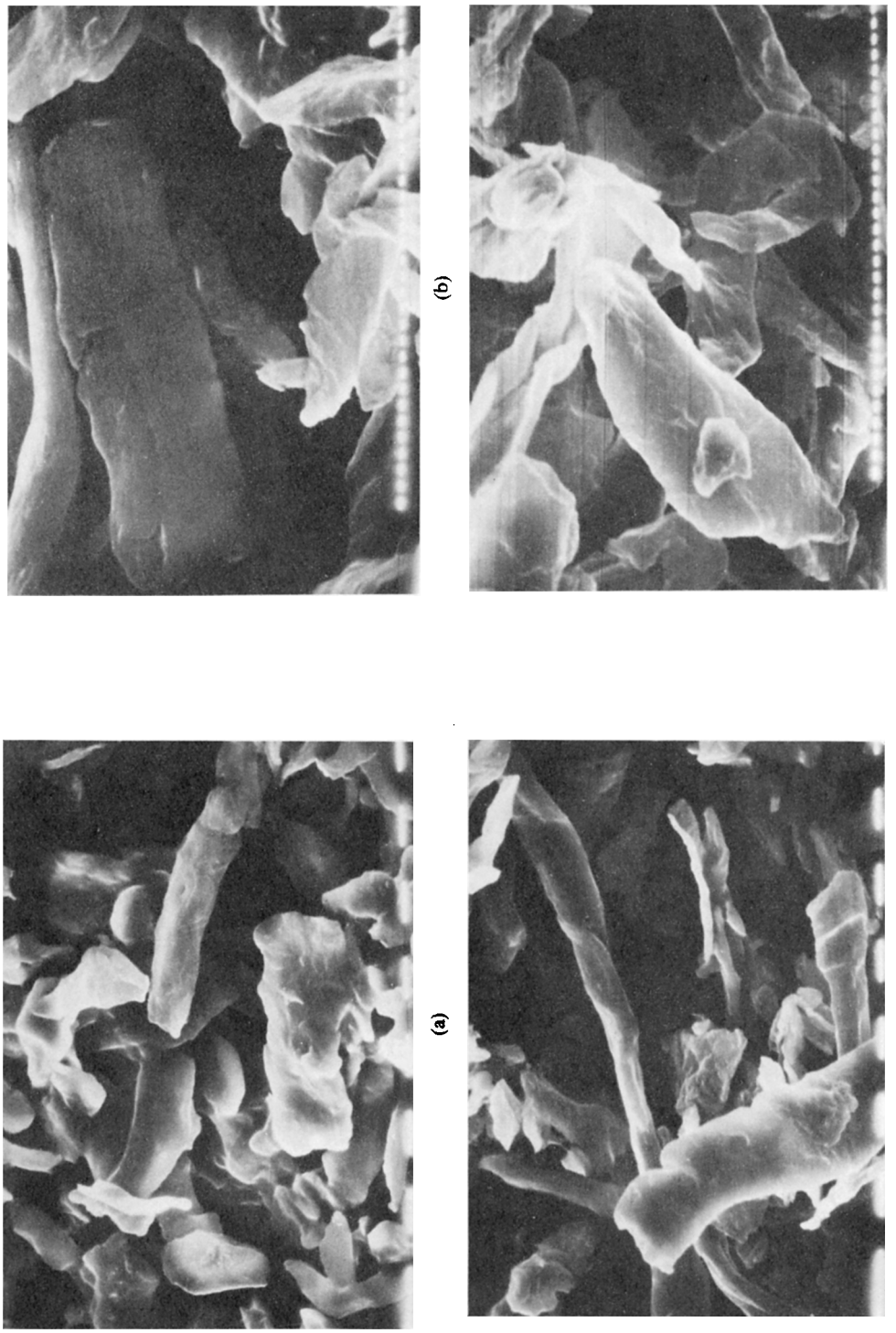

Fig. 15. Scanning electron micrographs of cellulose phosphate, (a) ×800, (b) ×1600, and cellulose phosphate heated for 15 min at (c) 140°C, ×800, (d) 140°C, ×1600, (e) 180°C, ×800, (f) 180°C, ×1600, (g) 260°C, ×800, and (h) 260°C, ×1600.

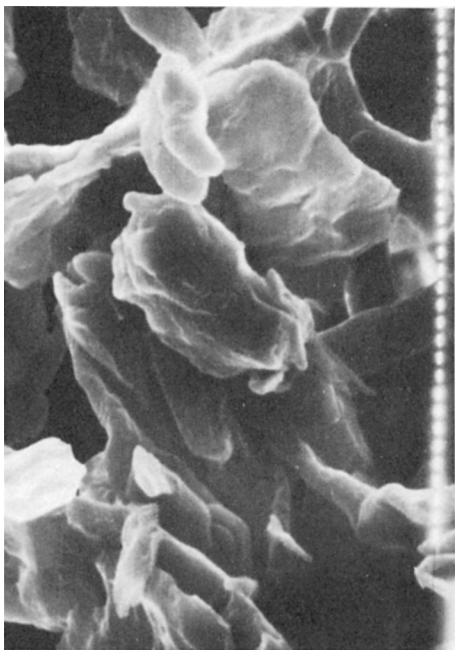

(f)

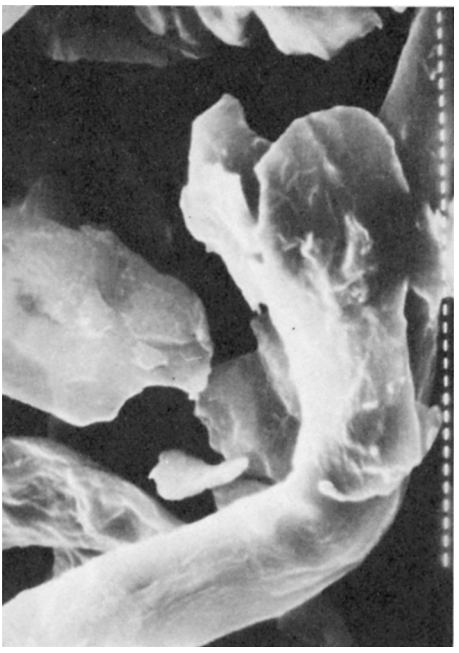

(h)

(e)

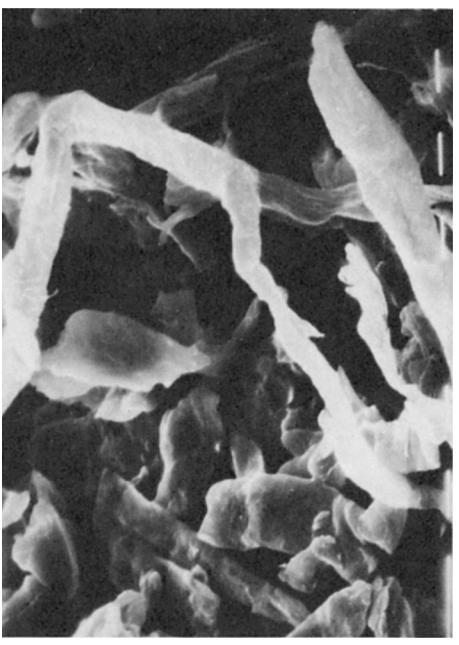

(g)

Fig. 15. *(Continued from the previous page.)*

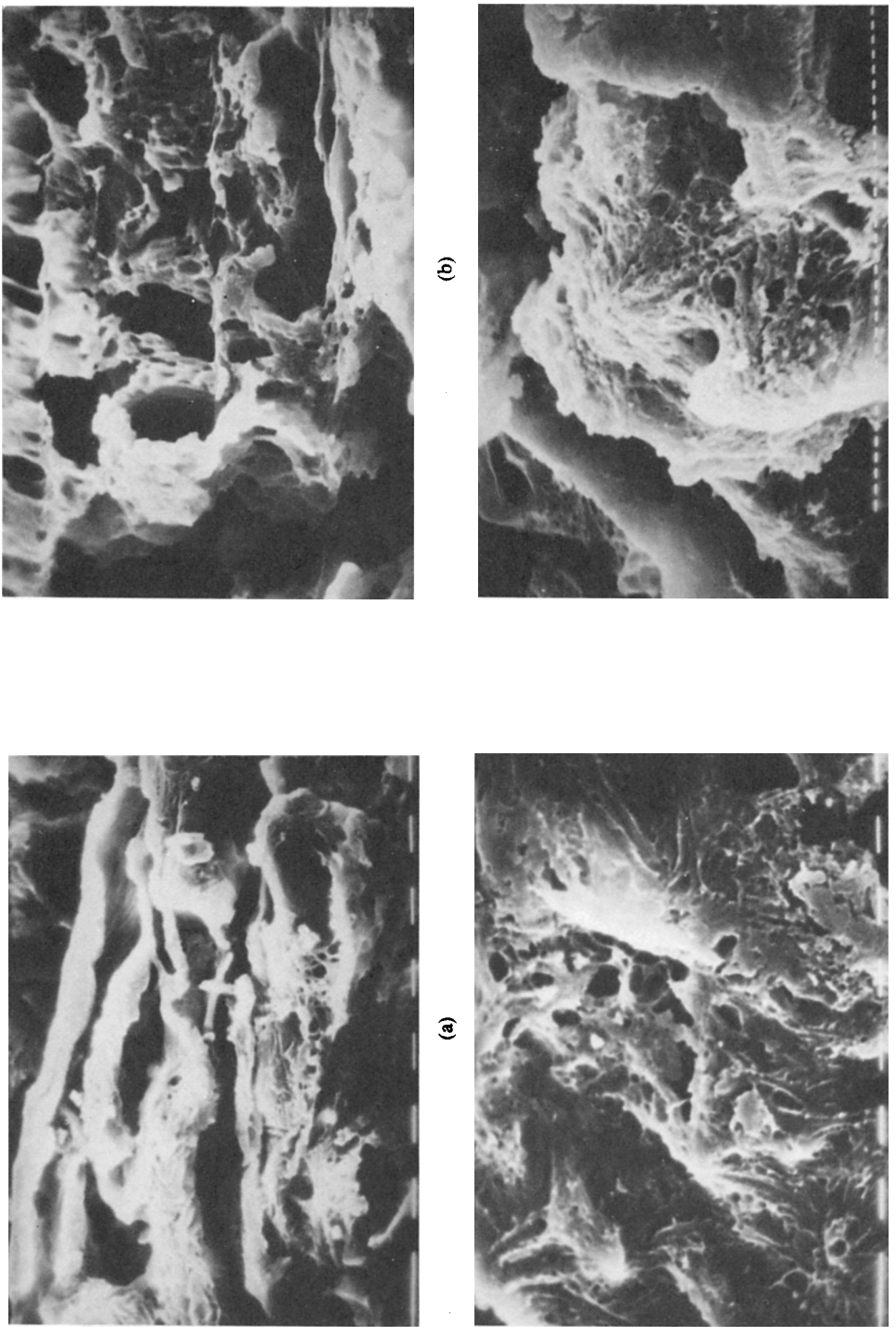

Fig. 16. Scanning electron micrographs of cellulose carbanilate, (a) ×800, (b) ×1600, and cellulose carbanilate heated for 15 min at (c) 250°C, ×800, (d) 250°C, ×1600, (e) 300°C, ×800, (f) 300°C, ×1600, (g) 350°C, ×800, and (h) 350°C, ×1600.

(f)

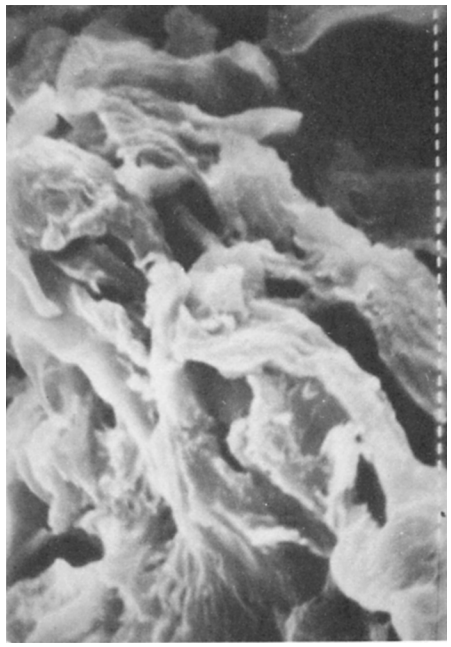

(h)

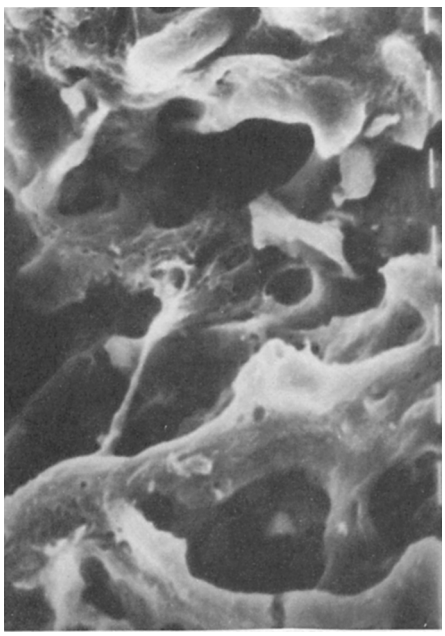

(e)

(g)

Fig. 16. *(Continued from the previous page.)*

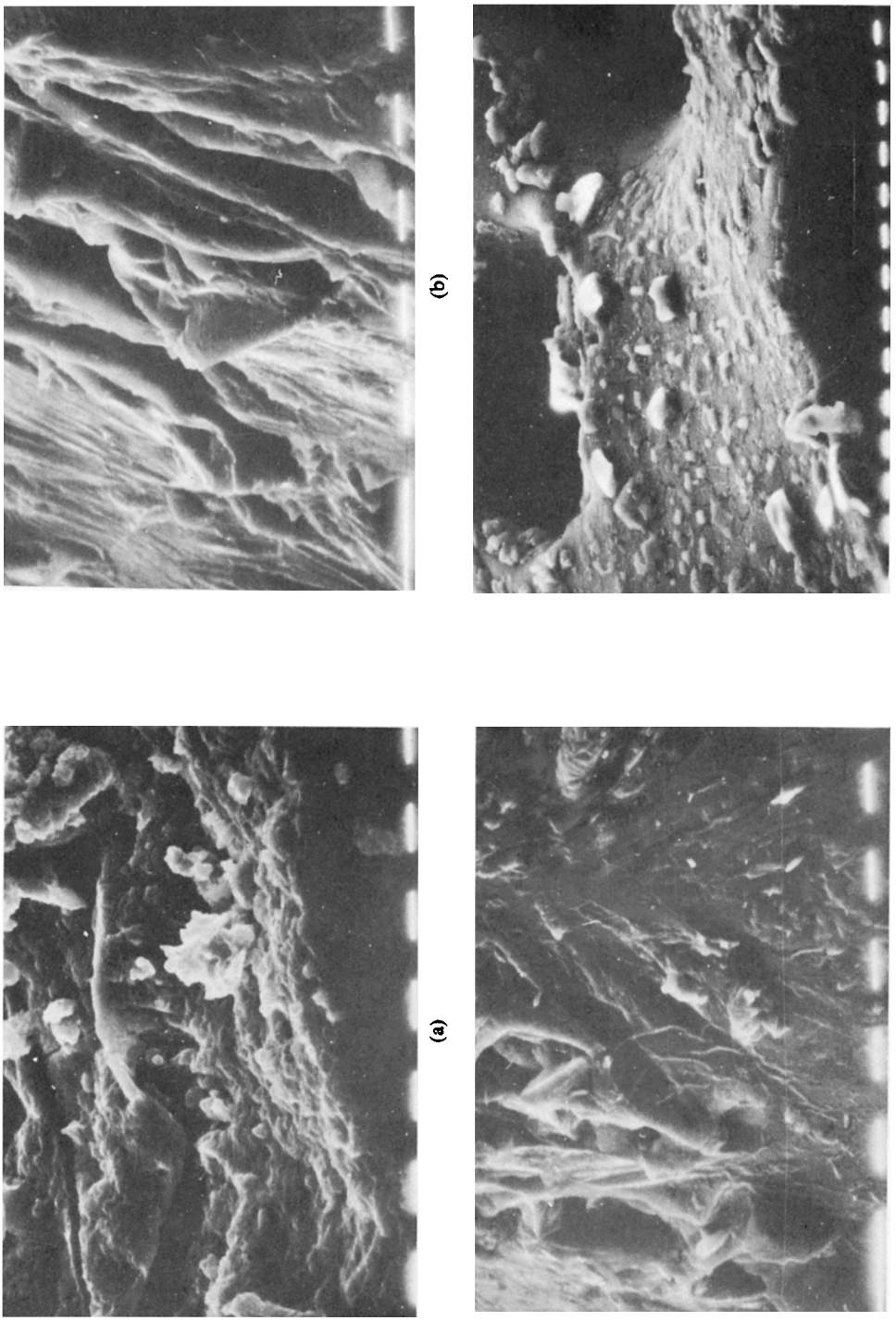

Fig. 17. Scanning electron micrographs of cellulose tosylate, (a) ×800, and cellulose tosylate heated for 15 min at (b) 150°C, ×800, (c) 175°C, ×800, and (d) 200°C, ×800.

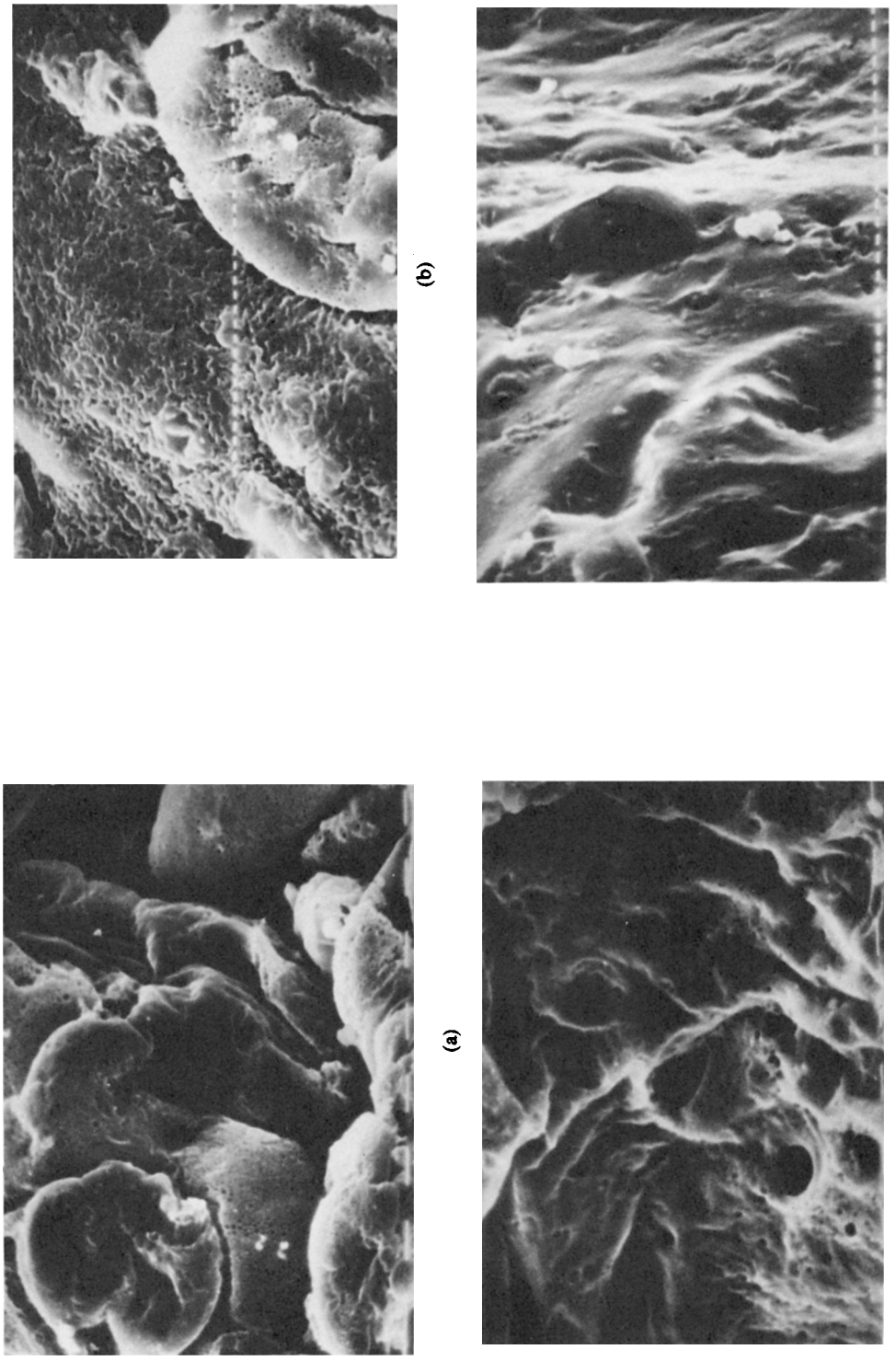

Fig. 18. Scanning electron micrographs of chlorodeoxycellulose, (a) ×800, (b) ×1600, and chlorodeoxycellulose heated for 15 min at (c) 190°C, ×800, (d) 190°C, ×1600, (e) 200°C, ×800, (f) 200°C, ×1600, (g) 250°C, ×800, and (h) 250°C, ×1600.

(f)

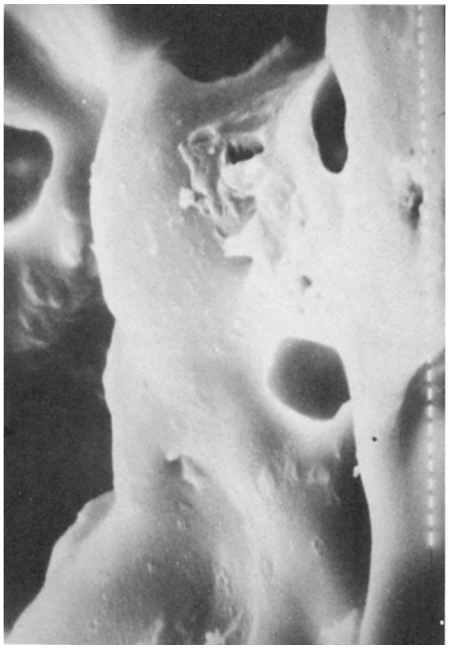

(h)

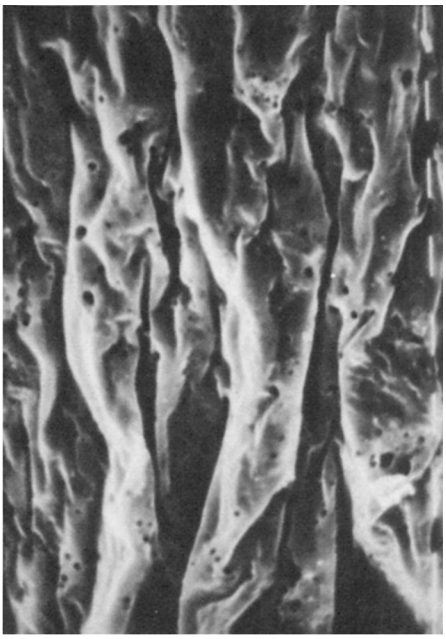

(e)

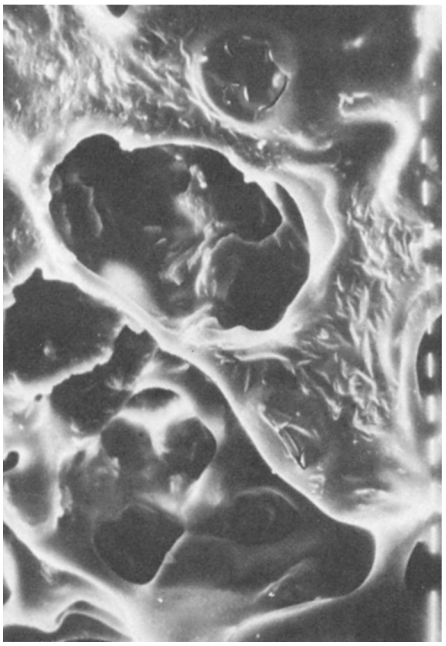

(g)

Fig. 18. *(Continued from the previous page.)*

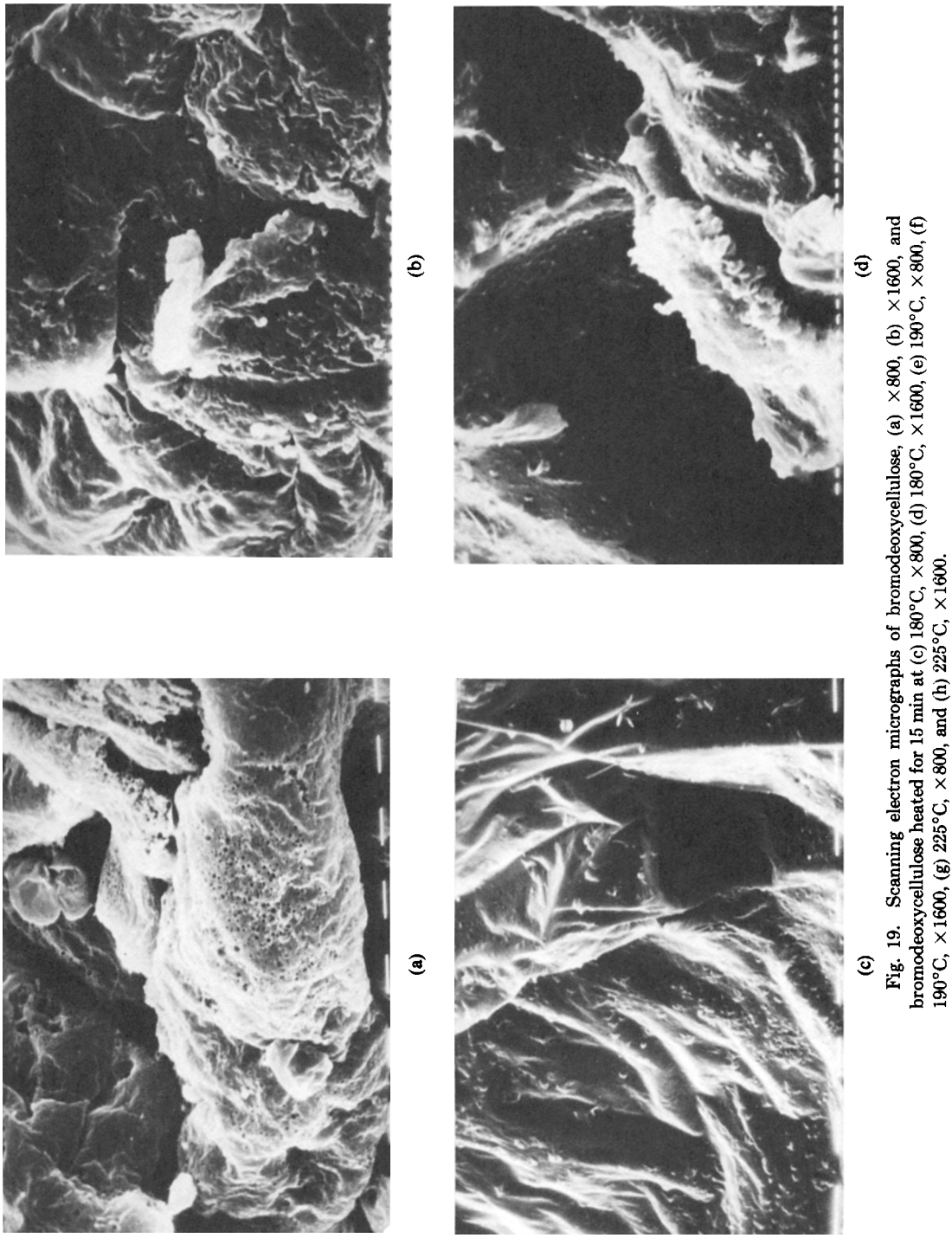

Fig. 19. Scanning electron micrographs of bromodeoxycellulose, (a) ×800, (b) ×1600, and bromodeoxycellulose heated for 15 min at (c) 180°C, ×800, (d) 180°C, ×1600, (e) 190°C, ×800, (f) 190°C, ×1600, (g) 225°C, ×800, and (h) 225°C, ×1600.

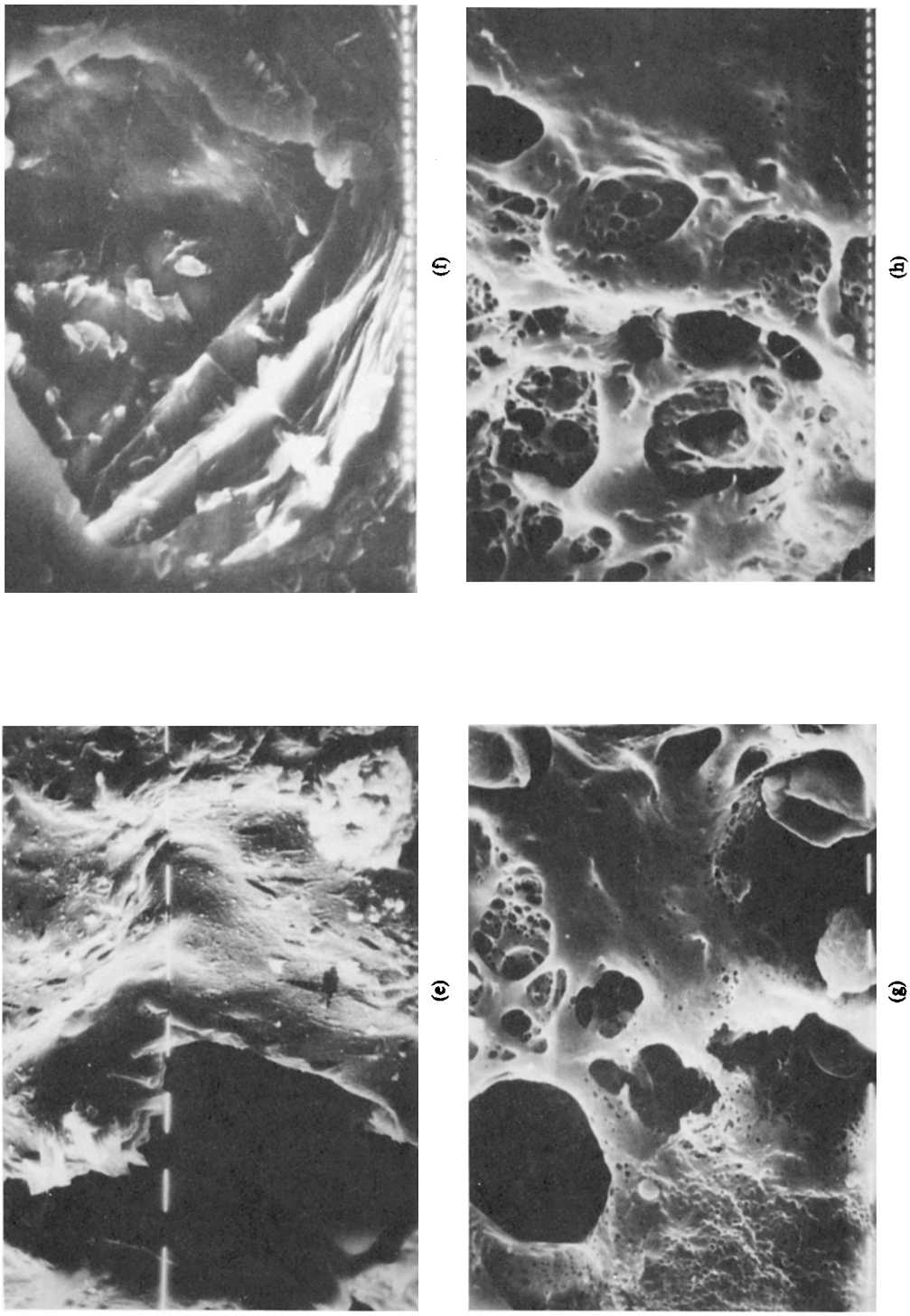

Fig. 19. (*Continued from the previous page.*)

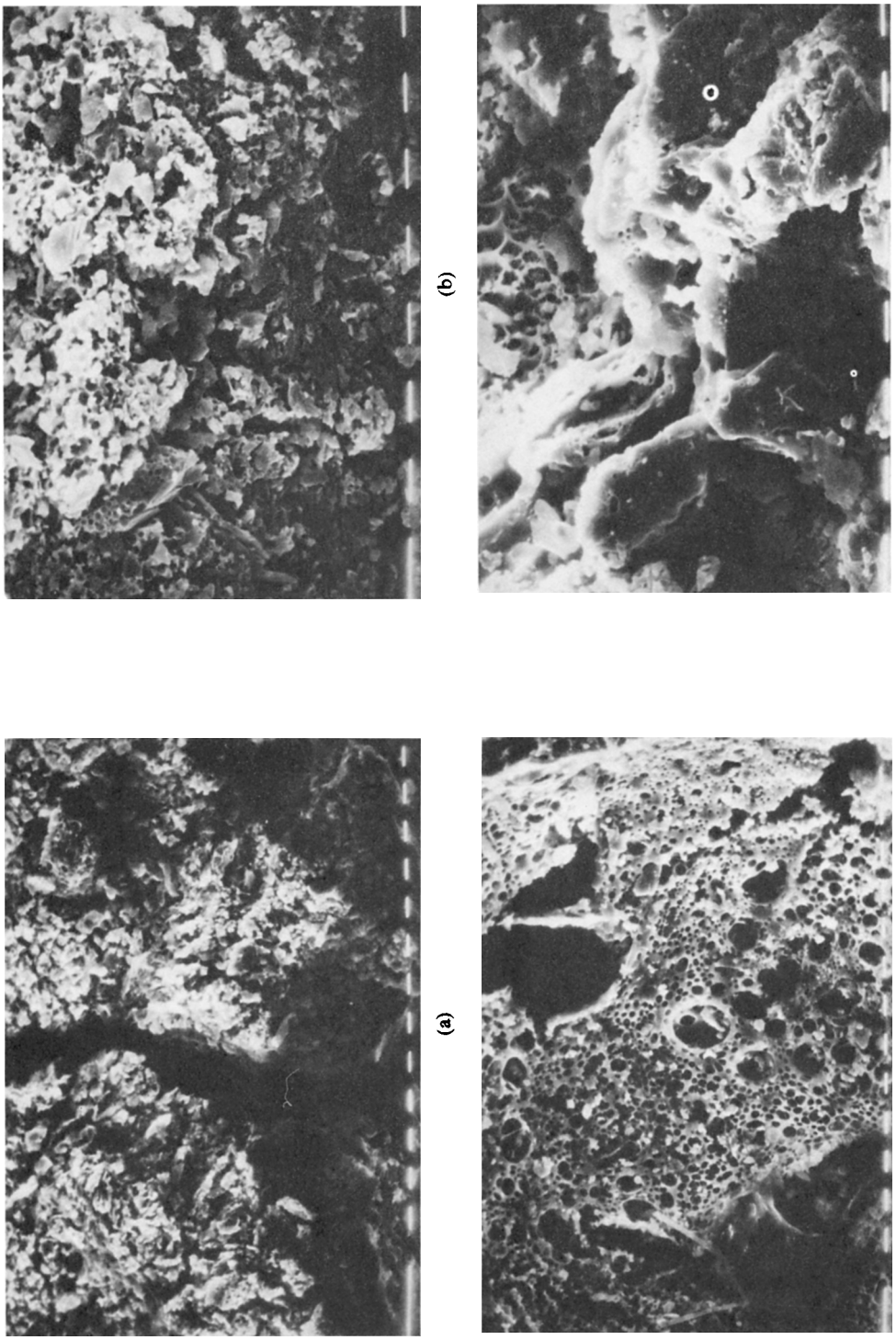

Fig. 20. Scanning electron micrographs of iododeoxycellulose, (a) ×400, (b) ×800, and iododeoxycellulose heated for 15 min at (c) 170°C, ×400, (d) 170°C, ×800, (e) 180°C, ×400, (f) 180°C, ×800, (g) 200°C, ×400, and (h) 200°C, ×800.

(f)

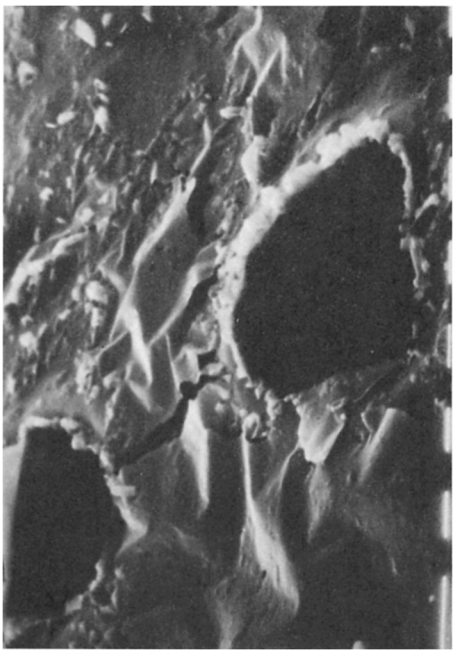

(h)

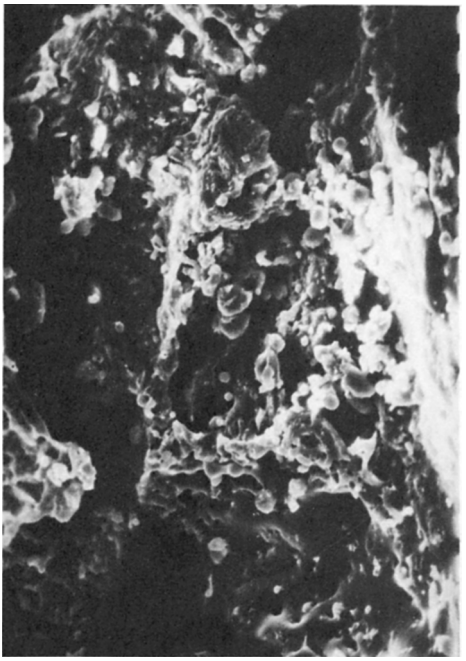

(e)

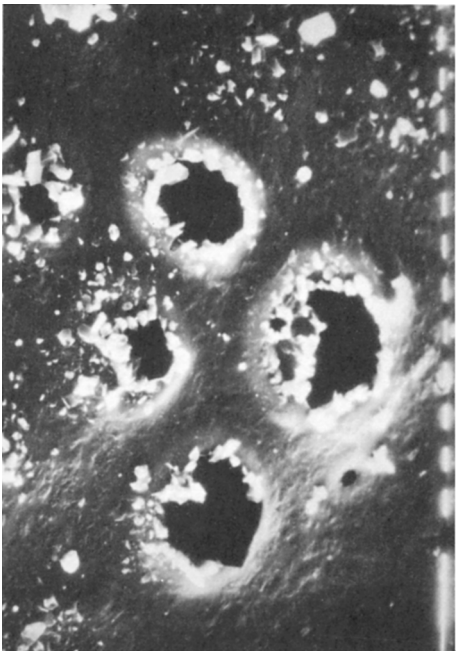

(g)

Fig. 20. *(Continued from the previous page.)*

the gaseous products seem to be evolved as big pits are visible, on the film surface.

For chlorodeoxycellulose, there is massive degradation in the fibrous structure of cellulose as no fibrillar structure is discernible in the SEM micrographs at ×800 and ×1600 magnifications [Fig. 18(a–b)]. When this sample is heated up to 190°C for 15 min [Fig. 18(c–d)], the structure tends to crosslink after dehydrohalogenation and detosylation with a corresponding mass loss of 10% in TG curve. At 200°C (mass loss 24.5%), the SEM micrographs [Fig. 18(e–f)] show tendency of alignment of fibers and film formation with small pits indicating the evolution of gas at this temperature. The evolution of gaseous products and tendency of film formation with big pits continues to increase with the rise in temperature as observed in the SEM micrographs at ×800 and ×1600 magnifications [Fig. 18(g–h)] for sample heated at 250°C for 15 min.

The SEM micrographs at ×800 and ×1600 magnifications of bromodeoxycellulose also show the disappearance of the fibrils with considerable degradation at microfibrillar sites [Fig. 19(a–b)]. On heating at 180°C for 15 min (corresponding to a mass loss of 7.4% in TG curve) the micrographs show the occurrence of crosslinking [Fig. 19(c–d)]. At 190°C, alignment in fibers and film formation are evidenced from the micrographs shown in Figure 19(e–f). At higher temperatures, (i.e. 225°C), the micrographs exhibit film formation with considerable pitting and evolution of gaseous products [Fig. 19(g–h)].

The original sample of iododeoxycellulose shows practically no fibrillar structure [Fig. 20(a–b)]. On heat treatment at 170°C for 15 min, the compound shows crosslinking with small pits [Fig. 20(c–d)]. Further, on heating at 180°C, the sample exhibits tendency to film formation with evolution of gaseous products [Fig. 20(e–f)]. Large pits and film formation are visible in the SEM micrographs obtained at 200°C [Fig. 20(g–h)].

One of the authors (R. K. J.) is thankful to the United States Department of Agriculture for providing a research associateship.

References

1. R. M. Aseeva and G. E. Zaikov, in *Developments and Stabilisation of Polymers*, Vol. 7, Applied Science Publishers Ltd., London, 1984, p. 233.
2. R. G. Bauer, *J. Fire Retardant Chem.*, **5**, 200 (1978).
3. P. D. Garn and C. L. Denson, *Text. Res. J.*, **47**, 485 (1977).
4. P. D. Garn and C. L. Denson, *Text. Res. J.*, **47**, 535 (1977).
5. J. W. Lyons, *J. Fire Flamm.*, **1**, 302 (1970).
6. F. Shafizadeh, P. S. Chin, and W. F. DeGroot, *J. Fire Flamm. Fire Retardant Chem.*, **2**, 195 (1975).
7. G. C. Tesoro, S. B. Sello, and J. J. Willard, *Text. Res. J.*, **39**, 180 (1969).
8. K. Katsuura and N. Inagaki, *J. Appl. Polym. Sci.*, **22**, 679 (1978).
9. H. Takaku, Y. Shimada, and K. Aoshima, *Chem. Pharm. Bull.*, **21**, 2068 (1973).
10. E. Heuser, M. Heath, and W. M. H. Shockley, *J. Am. Chem. Soc.*, **72**, 670 (1950).
11. W. A. Pons, Jr. and J. D. Guthrie, *Ind. Engng. Chem.*, **18**, 184 (1946).
12. H. T. Clarke, Ed., *Handbook of Organic Analysis*, Orient-Longmans Ltd., London, 1970, p. 308.
13. W. K. Tang, in *Differential Thermal Analysis*, Vol. 2, R. C. Mackenzie, ed., Academic Press, London and New York, 1972, p. 523.
14. J. M. Cowie and S. A. E. Henshall, *Eur. Polym. J.*, **12**, 215 (1976).

15. F. Shafizadeh, Y. Z. Lai, and C. R. McIntyre, *J. Appl. Polym. Sci.*, **22**, 1183 (1978).
16. A. Broido, *J. Polym. Sci.*, Part A-2, **7**, 1761 (1969).
17. J. E. Wertz and J. R. Bolton, *Electron Spin Resonance*, McGraw-Hill, New York, 1972, p. 32.
18. N.-S. Hon, *J. Polym. Sci. Polym. Chem. Ed.*, **13**, 1933 (1975).
19. J. C. Arthur, Jr. and O. Hinojosa, *J. Polym. Sci.*, Part C, **36**, 53 (1971).
20. O. Hinojosa, J. C. Arthur, Jr., and T. Mares, *Text. Res. J.*, **43**, 609 (1973).
21. I. Hardin and L. Slaten, *Preprints, ACS Div. of Organ. Coatings Plast. Chem.*, **36**, 462 (1976).
22. A. Granzow, *Accts. Chem. Res.*, **11**, 177 (1978).
23. R. K. Jain, K. Lal, and H. L. Bhatnagar, *J. Appl. Polym. Sci.*, **30** 897 (1985).
24. G. C. Tesoro, S. B. Sello, and J. J. Willard, *Text. Res. J.*, **38**, 245 (1968).
25. J. E. Hendrix, G. L. Drake, Jr., and R. H. Barker, *J. Appl. Polym. Sci.*, **16** 257 (1972).
26. A. J. Papa, *Ind. Eng. Chem. Prod. Res. Dev.*, **9**, 478 (1970).
27. A. J. Papa and W. R. Proops, *J. Appl. Polym. Sci.*, **16**, 2361 (1972).
28. A. Broido and M. A. Nelson, *Combust. Flame*, **24**, 263 (1975).
29. R. C. Weast, ed., *CRC Handbook of Chemistry and Physics*, 59 ed., CRC Press, Inc., Boca Raton Florida, 1978–1979, p. F-219.
30. F. Shafizadeh, Y. Z. Lai, and C. R. Nelson, *J. Appl. Polym. Sci.*, **20**, 139 (1976).

Received May 5, 1986
Accepted June 30, 1986